Marine Geology 432 (2021) 106383

Contents lists available at ScienceDirect

Marine Geology

journal homepage: www.elsevier.com/locate/margo

Submarine morphology of the Comoros volcanic archipelago

A. Tzevahirtzian [a,b,*], S. Zaragosi [b], P. Bachèlery [c], L. Biscara [d], E. Marchès [d]

[a] Dipartimento di Scienze della Terra e del Mare (DiSTeM), Università degli Studi di Palermo, via Archirafi 20-22, 90123 Palermo, Italy
[b] EPOC, UMR CNRS 5805, Université de Bordeaux, allée Geoffroy Saint-Hilaire, CS 50023, F-33615 Pessac, Cedex, France
[c] Université Clermont Auvergne, CNRS, IRD, OPGC, Laboratoire Magmas et Volcans, 6 avenue Blaise Pascal, 63178 Aubière, France
[d] SHOM, 13 rue du Chatellier, CS 92803, F-29228 Brest, Cedex 2, France

ARTICLE INFO

Keywords:
Comoros archipelago
Morpho-bathymetry
Submarine volcanism
Volcanic ridges
Volcanic cones
Mounds
Mass slope instabilities

ABSTRACT

A detailed morpho-bathymetric study of the Comoros archipelago, based on mostly unpublished bathymetric data, provides a first glimpse into the submarine section of these islands. It offers a complete view of the distribution of volcanic structures around the archipelago, allowing to discuss the origin and evolution of this volcanism. Numerous volcanic cones and erosional-depositional features have been recognized throughout the archipelago. The magmatic supply is focused below one or several volcanoes for each island, but is also controlled by lithospheric fractures evidenced by volcanic ridges, oriented along the supposed Lwandle-Somali plate boundary. Massive mass-wasting morphologies also mark the submarine flanks of each island. Finally, the submarine geomorphological analysis made possible to propose a new scheme for the succession of the island's growth, diverging from the east-west evolution previously described in the literature.

1. Introduction

From the ocean floor to their top, oceanic hot spot islands form very large reliefs and can be considered as the largest mountains on Earth (Huff and Owen, 2013). Their morphology results from the juxtaposition of both endogenous (mantle and crustal geodynamic and tectonic, melt generation and differentiation, intrusive growth…) and exogenous (eruptive regime and dynamism, gravitational instabilities, erosion, sediment transport, weathering…) processes, and consequently provides good insights into how oceanic islands grow and evolve (Bachèlery and Villeneuve, 2013). The submarine flanks of these edifices, by far larger than their emerged counterpart, remain however less studied given the difficulties inherent to their observation and the costly resources to be deployed. Since pioneering work (Moore, 1964; Moore and Fiske, 1969; Spiess et al., 1969), significant progress has been made in mapping the submarine slopes of oceanic volcanoes and understanding their development. They are shaped by two main groups of processes: growth by primary volcanic emissions (lava flows, pyroclastics, hyaloclastites) and intrusions, and destruction by gravity-driven instabilities (landslides, slumps, catastrophic debris avalanches, density flows) and shallow-water erosion (waves, sea-level changes, heavy rains) (e.g., Holcomb and Searle, 1991; Ramalho et al., 2013; Saint-Ange et al., 2013; Staudigel and Koppers, 2015; Casalbore, 2018). Primary volcanic structures most often reflect the interactions between magmatism and tectonics (Binard et al., 1992; Hekinian et al., 2003; Devey et al., 2003; Rubin et al., 2012) and the degree of maturity of the volcano (Mitchell, 2001; Acosta et al., 2003; Casalbore et al., 2015; Clague et al., 2019). As such, the morpho-structural analysis of volcanic edifices can provide insights for evaluating local geodynamics and volcano's evolutions.

Gravity-driven instabilities have been recognized as a common process in the building of oceanic islands, including many basaltic intraplate volcanoes. Two main types of landslides are generally covering large portions of the volcanoes' submarine flanks: catastrophic debris avalanches (fast-moving landslides) and more coherent slumps (Moore et al., 1989; McGuire, 1996; Krastel et al., 2001a; Masson et al., 2002; Mitchell et al., 2002; Coombs et al., 2004; Masson et al., 2008; Oehler et al., 2008; Le Friant et al., 2011; Mitchell et al., 2013; Denlinger and Morgan, 2014; Hunt and Jarvis, 2017). Erosion forms gullies and canyons, and feed fan-shaped turbidite deposits that may widely spread on the abyssal plain (Krastel et al., 2001b; Sisavath et al., 2011; Mazuel et al., 2016). As volcanic activity declines, the combined effects of erosion and subsidence reduce the height of the volcanic edifice and led to the formation of an insular shelf (Quartau et al., 2014; Romagnoli et al., 2018). In tropical environment, the growth of carbonate submarine terraces may give information on the chronological evolution of the islands (Puga-Bernabéu et al., 2016; Counts et al., 2018).

* Corresponding author at: Dipartimento di Scienze della Terra e del Mare (DiSTeM), Università degli Studi di Palermo, via Archirafi 20-22, 90123 Palermo, Italy.
E-mail address: athina.tzevahirtzian@unipa.it (A. Tzevahirtzian).

https://doi.org/10.1016/j.margeo.2020.106383
Received 23 July 2020; Received in revised form 19 November 2020; Accepted 24 November 2020
Available online 4 December 2020

In comparison to other volcanic archipelagoes, such as Hawaii, Canaries or Azores, Comoros Islands are poorly known, and the seabed of the region is very little studied yet. This is an obstacle in the comprehension of the origin of the Comorian volcanism, which explains the open debate for 50 years. The Comoros Islands display the different erosional stages specific to volcanic dynamic (Darwin, 1842). The islands have been almost exclusively studied in their terrestrial part, except for Mayotte due to its lagoon and its developed barrier reef (Guilcher et al., 1965; Zinke et al., 2003a & b; Audru et al., 2006). Studies on the geology, geochronology and the archipelago's volcanism have been made, but many questions remain to be resolved (Esson et al., 1970; Hajash and Armstrong, 1972; Emerick and Duncan, 1982; Nougier et al., 1986; Bachèlery and Coudray, 1993; Späth et al., 1996; Michon, 2016).

This paper aims to document the geomorphology of the submarine part of the Comoros archipelago, emphasizing the juxtaposition of erosive-depositional and volcanic structures. Based on our morphological analysis, the origin and evolution of the Comoros archipelago are discussed.

2. Geological background

2.1. Regional context of volcanism

The Comoros archipelago includes the islands of Grande Comore, Anjouan, Mohéli and Mayotte, extending over 270 km in the Somali-Comoros Basin, at the northern entrance of the Mozambique Channel in the western Indian Ocean (Fig. 1A, B).

The Comoros volcanic edifices stand on a tectonically and seismically active zone, extending approximately E-W, from the northern end of the Davie Ridge to the north of Madagascar (Fig. 1A). It is considered as the potential diffuse Lwandle-Somali sub-plate boundary (Rindraharisaona et al., 2013; Michon, 2016; Stamps et al., 2018; Famin et al., 2020), and part of the SE seaward extension of the East African Rift System (Kusky et al., 2010; Franke et al., 2015; Deville et al., 2018; Courgeon et al., 2018; O'Connor et al., 2019).

From the Jurassic to Early Cretaceous, the Gondwana breakup was marked by NE-SW oriented seafloor ridges allowing the gradual opening of Somali and Mozambique basins, and the southern migration of Madagascar (Segoufin and Patriat, 1980; Coffin and Rabinowitz, 1987; Key et al., 2008; Emmel et al., 2011; Davis et al., 2016; Mueller and Jokat, 2019; Thompson et al., 2019). During the Cenozoic, the East African Rift System develops in two major branches (Malod et al., 1991; Mpanda, 1997; Chorowicz, 2005; Franke et al., 2015), and extends offshore from the Miocene and then the Pliocene (Mougenot et al., 1986; Franke et al., 2015; Macgregor, 2015). Several submarine grabens characterize the offshore branch of the rift and a major structural high, the Davie Ridge (Raillard, 1990; Chorowicz, 2005; see also Franke et al., 2015, Fig. 1). Since the Pleistocene, this offshore branch extends southwards through the reactivation of the Davie Ridge in the southern part of the Sakalaves Seamounts and possibly up to the Quathlamba Seismic Axis (Franke et al., 2015; Courgeon et al., 2018).

The volcanic activity of the Comoros Islands began since the Mio-Pliocene (Esson et al., 1970; Hajash and Armstrong, 1972; Emerick and Duncan, 1982; Pelleter et al., 2014). Only few absolute ages are available in the literature, obtained from the emerged part of each island: Mayotte 10.6 ± 0.5 Ma to ~6 ka, Anjouan and Mohéli 11.1 ± 0.5 Ma to 0.36 ± 0.09 Ma and 5.0 ± 0.4 Ma to 0.48 ± 0.15 Ma, respectively, and Grande Comore 0.13 ± 0.02 Ma to present (Hajash and Armstrong, 1972; Emerick and Duncan, 1982; Nougier et al., 1986; Zinke et al., 2003a, 2005; Debeuf, 2004; Pelleter et al., 2014). Nougier et al. (1986) estimated the onset of the volcanism of Mayotte around 15–10 Ma, but according to Michon (2016), the volcanic activity of the Comoros archipelago is probably older and would have started in Mayotte 20 Ma ago, and then developed in Anjouan, Mohéli and Grande Comore almost simultaneously 10 Ma ago. From seismic stratigraphy, Leroux et al. (2020) confirm that the main volcanic phase of Mayotte occurred between ~15–20 Ma and ~ 3 Ma. Today's active volcanism has been described for the island of Grande Comore and offshore Mayotte. On Grande Comore, Karthala's volcano most recent eruptions occurred in 1991, and from 2005 to 2007 (Bachèlery et al., 1995; Bachèlery et al., 2016). A seismic crisis and a submarine volcanic eruption began 50 km east of Mayotte in mid-May 2018. Activity is ongoing at the time of writing (Feuillet et al., 2019; Lemoine et al., 2020; Cesca et al., 2020).

The Comoros volcanism has been interpreted in different ways. It was regarded as hotspot-related (Emerick and Duncan, 1982; Emerick, 1985; Hajash and Armstrong, 1972; Morgan, 1972; Späth et al., 1996; Class et al., 1998) or due to deep lithospheric faults (Upton, 1982; Nougier et al., 1986), in relation to the East African Rift System (Michon, 2016; O'Connor et al., 2019; Famin et al., 2020). The most recent work tends to consider the Comoros archipelago as an E-W right-lateral shear zone and a diffuse boundary between the Lwandle and Somali plates, rather than the surface expression of a deep mantle plume (Michon, 2016; Famin et al., 2020).

2.2. Geological framework of the islands

Grande Comore (Fig. 2) is the largest island (1100 km^2) of the Comoros archipelago. Three volcanic massifs shape the island (Bachèlery and Coudray, 1993; Bachèlery et al., 2016). Karthala (2360 m) is a frequently active shield volcano. On the northern part of the island, La Grille Massif was mostly active during the Pleistocene (Bachèlery and Coudray, 1993; Bourhane et al., 2016) and has erupted several times in the last few thousand years (1300 ± 65 years BP and 740 ± 130 years BP in Bachèlery and Coudray, 1993; Bachèlery et al., 2016). Unusual steep slopes (locally >30°) on Karthala and La Grille flanks have been interpreted as landslide scars (Bachèlery et al., 2016). Recent eruptive fissures and cinder cones observed on Karthala and La Grille volcanoes define volcanic rift zones with N-S and NW-SE orientations (Fig. 2A - Bachèlery et al., 2016). M'Badjini Massif is considered to be the oldest volcanic center of Grande Comore (Bachèlery and Coudray, 1993). A discontinuous fringing reef is present all around the coastline of Grande Comore (Guilcher et al., 1965).

Mohéli (Fig. 3) is the smallest island of the Comoros archipelago (290 km^2) culminating at Mount M'Ze Koukoulé (790 m). Little is known about the geology of Mohéli. Nougier et al. (1986) proposed the existence of ancient series outcropping mainly in the west of the island, while the summits and the east of the island are covered by younger formations. Recent craters and lava flows define a WNW-ESE (N 115°) alignment that may correspond to an old volcanic rift zone (see Fig. 4 in Famin et al., 2020). A well-developed fringing reef is present all around the island (Guilcher et al., 1965).

Anjouan (Fig. 4) has a triangular shape of 424 km^2, with three peninsulas extending to the north, south and west. Esson et al. (1970) suggest that NW-SE and NNW-SSE oriented faults probably control its fairly rectilinear coastlines, while its northern concave-shaped coastline is associated with faults and local subsidence phenomena. The relief of Anjouan is very rugged and shaped by deep river erosion of the oldest basaltic sequences, with its highest peak, Mount N'Tingui, culminating at 1575 m (Esson et al., 1970). The oldest formations are mainly outcropping in the center of the island, while the peninsulas are covered with more recent series (Nougier et al., 1986; Famin et al., 2020). Well-preserved volcanic cones, corresponding to recent eruptions, form alignments (N105° and N152°) that roughly correspond to the main topographic crests of the island (see Fig. 4 in Famin et al., 2020). These alignments are interpreted as volcanic rift zones. The island is bordered by fringing reefs on two-thirds of its periphery (Guilcher et al., 1965).

Mayotte (Fig. 5) consists of two main islands, Grande Terre and Petite Terre, and nearly 20 smaller islets (Guilcher et al., 1965). A unique mountain range and secondary massifs with steep slopes and narrow coastal plains mark its topography (Lachassagne et al., 2014). Mayotte is considered to be the result of subaerial volcanic activity since about 10

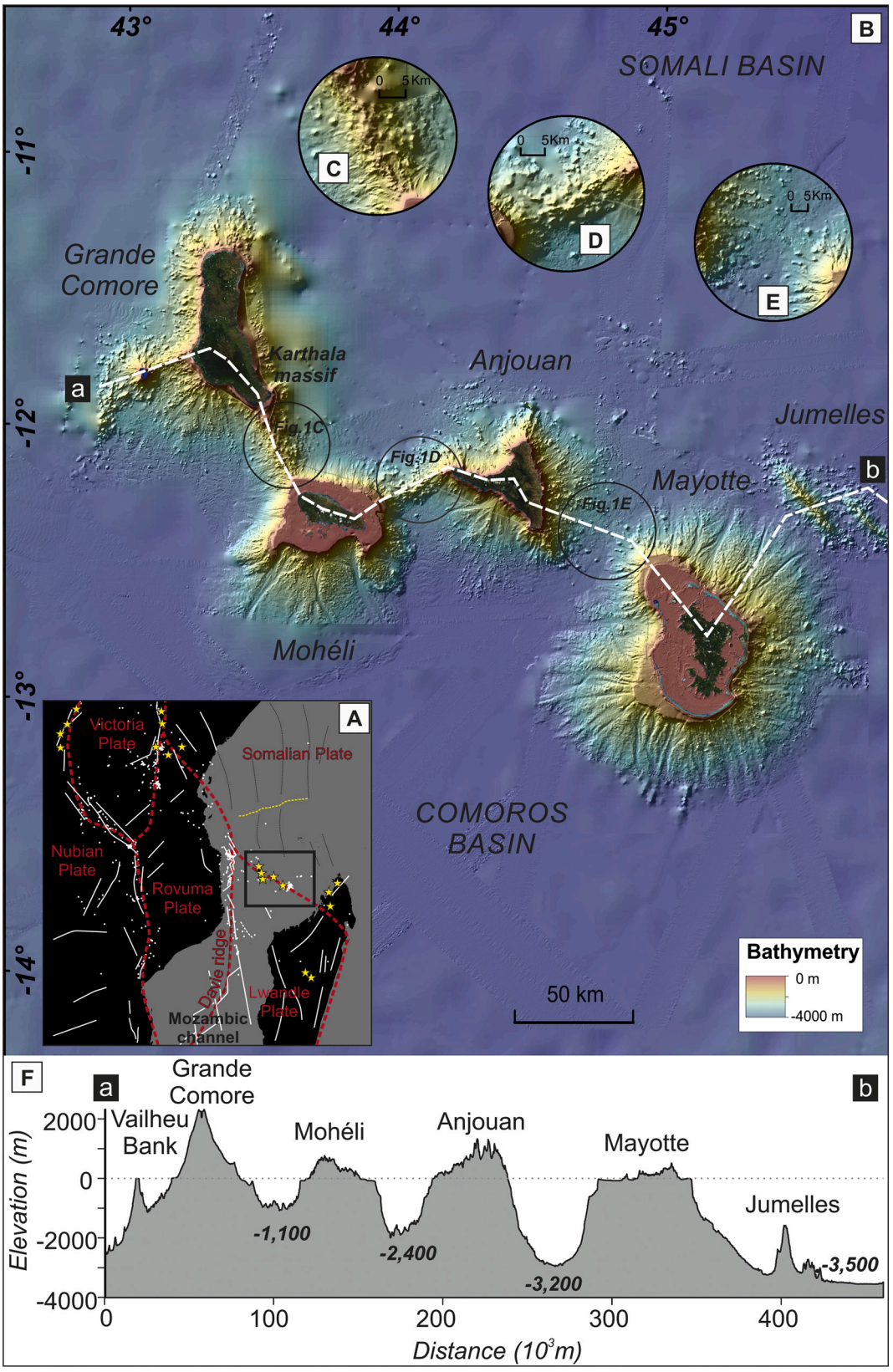

Fig. 1. (A) Location of the Comoros archipelago in the Mozambique Channel. (B) Bathymetry around the Comoros archipelago (sources: Gridded Bathymetry Chart of the Oceans - GEBCO 2008, MNT Shom). (C) Detailed view of the volcanic ridge between Grande Comore and Mohéli islands. (D) Detailed view of the volcanic ridge between Mohéli and Anjouan islands. (E) Detailed view of the volcanic ridge between Anjouan and Mayotte islands. (F) Topographic profile across the Comoros archipelago.

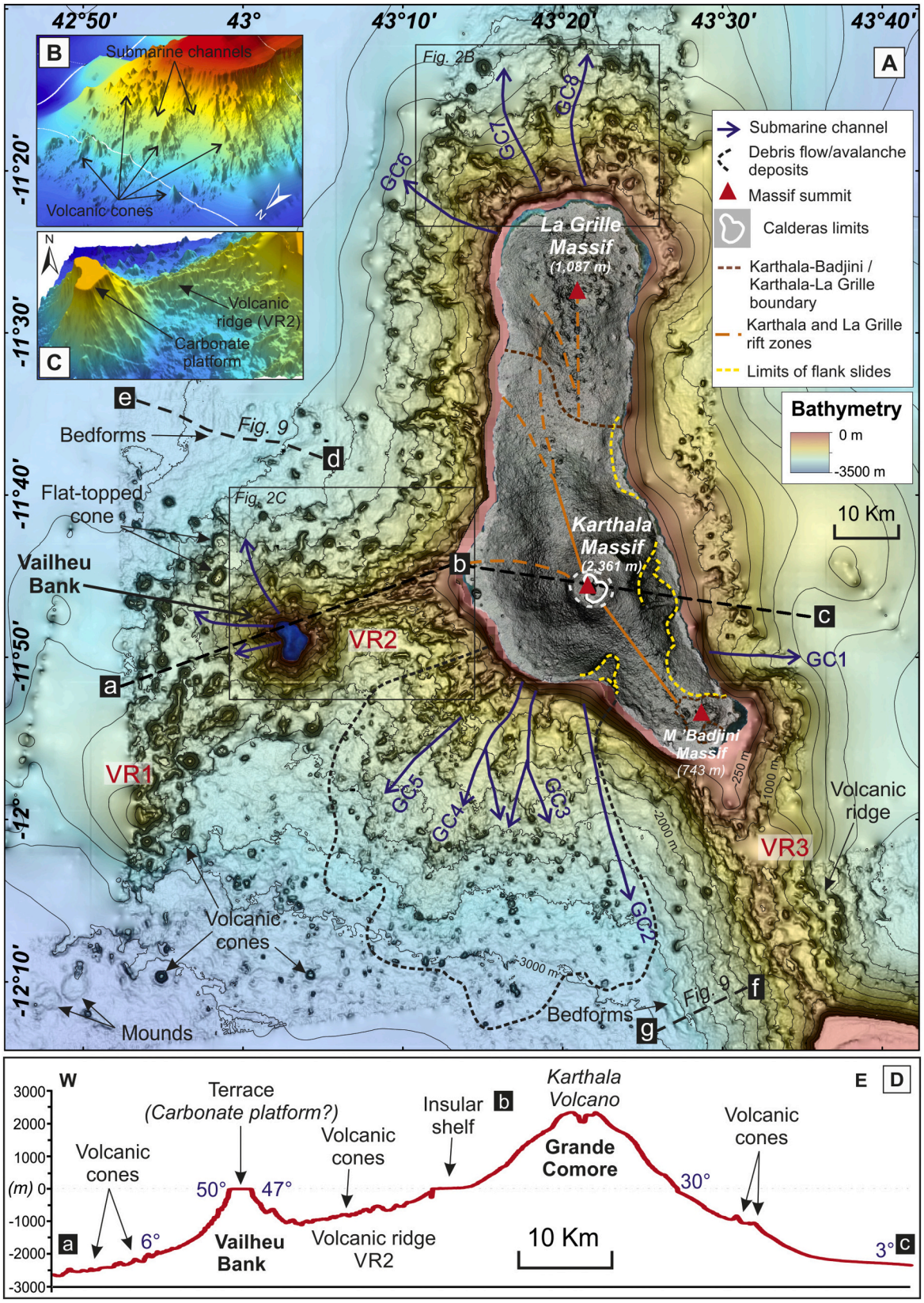

Fig. 2. (A) Morpho-bathymetric map of Grande Comore and Vailheu Bank (see location in Fig. 1B). Onshore rift zones and landslides are from Bachèlery et al. (2016). The location of the profiles across the bedform fields shown in Fig. 9 is indicated. (B) 3D underwater visualization of the channels and volcanic cones at the northern tip of Grande Comore (C) 3D visualization of Vailheu Bank and volcanic ridge VR2. (D) Bathymetric profile showing from west to east, Vailheu Bank and Grande Comore (a to c).

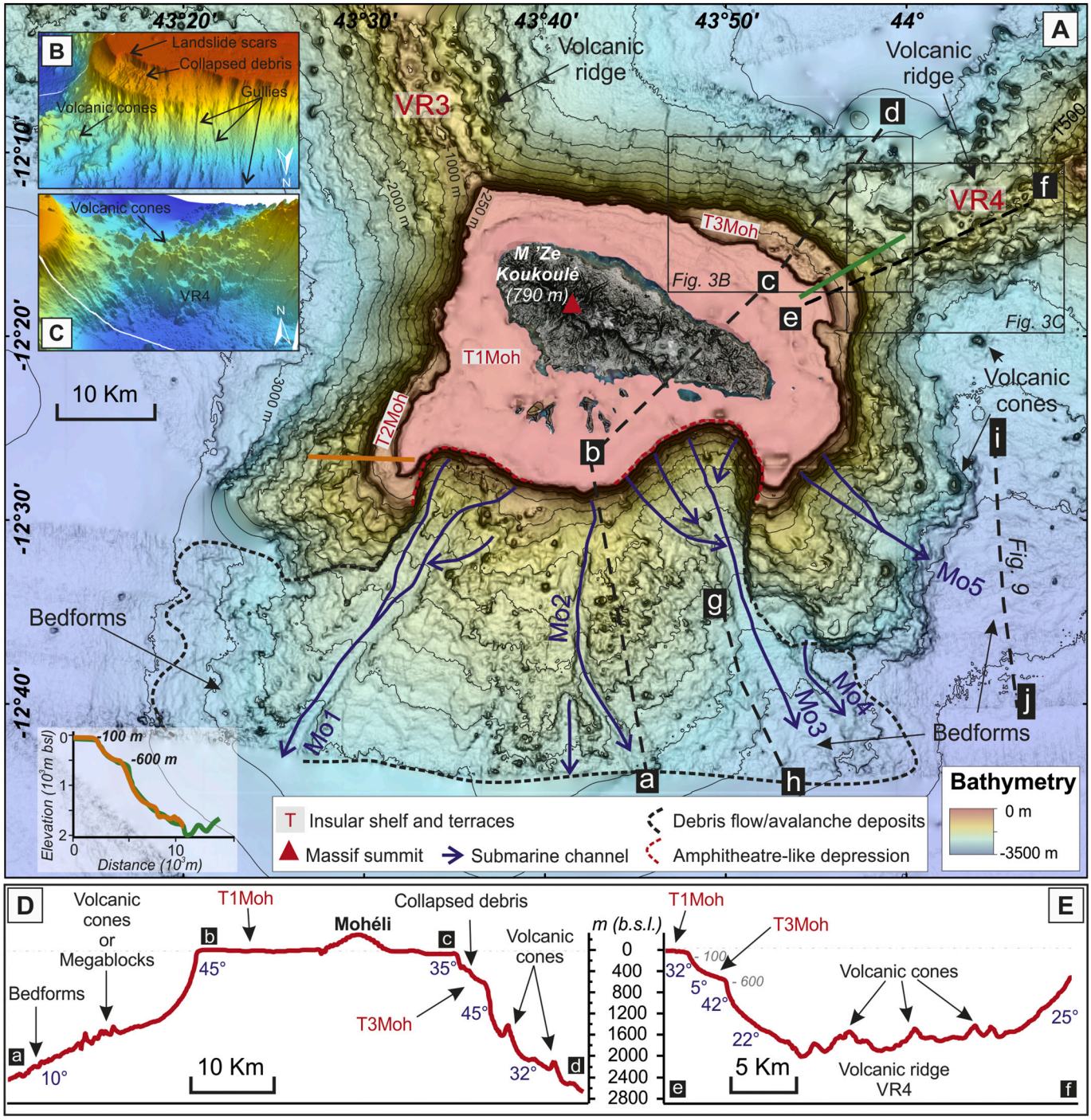

Fig. 3. (A) Morpho-bathymetric map of Mohéli (see location in Fig. 1B). Two bathymetric profiles intersecting the terraces T2Moh (in orange) and T3Moh (in green) are shown. The location of the profiles across the bedform fields shown in Fig. 9 is indicated. (B) Underwater 3D visualization of the submarine plateau and the terrace T3Moh. On T3Moh collapsed debris are visible. (C) 3D view of the volcanic ridge that connects the SE of Mohéli and Anjouan, characterized by a multitude of conical reliefs. (D) Bathymetric profile across the island including the insular shelf and the terrace T3Moh (a to d). (E) Bathymetric profile along the volcanic ridge VR4, between Mohéli and Anjouan (e-f). (For interpretation of the references to colour in this figure legend, the reader is referred to the web version of this article.)

Ma, with at least two Miocene to Pleistocene shield volcanoes (Southern complex and Northern complexes) on which more recent massifs (Digo and M'Tsapéré) have been built (Audru et al., 2006; Debeuf, 2011; Nehlig et al., 2013; Lacquement et al., 2013; Pelleter et al., 2014; Vittecoq et al., 2014). Audru et al. (2006) described normal faults along two main directions: N45° and N160-180°. Dykes are essentially observed along the northwestern coast with a dominant N150-160° orientation (Famin et al., 2020). No clear rift zone can be identified. During the last 20,000 yrs. (Last Glacial Maximum), the island has undergone a subsidence of 2.4–5 m (Camoin et Davies, 1998; Camoin et al., 2004), which corresponds to an average subsidence rate of 0.19 to 0.25 mm/year (Audru et al., 2006; Montaggioni and Martin-Garin, 2020). Mayotte has the largest barrier reef - lagoon complex in the Indian Ocean (Zinke et al., 2003a & b). The thick soils resulting from the laterite alteration of basaltic lavas (Guilcher et al., 1965), and the coastal indentations of the island linked to erosion, are also indicative of Mayotte's maturity.

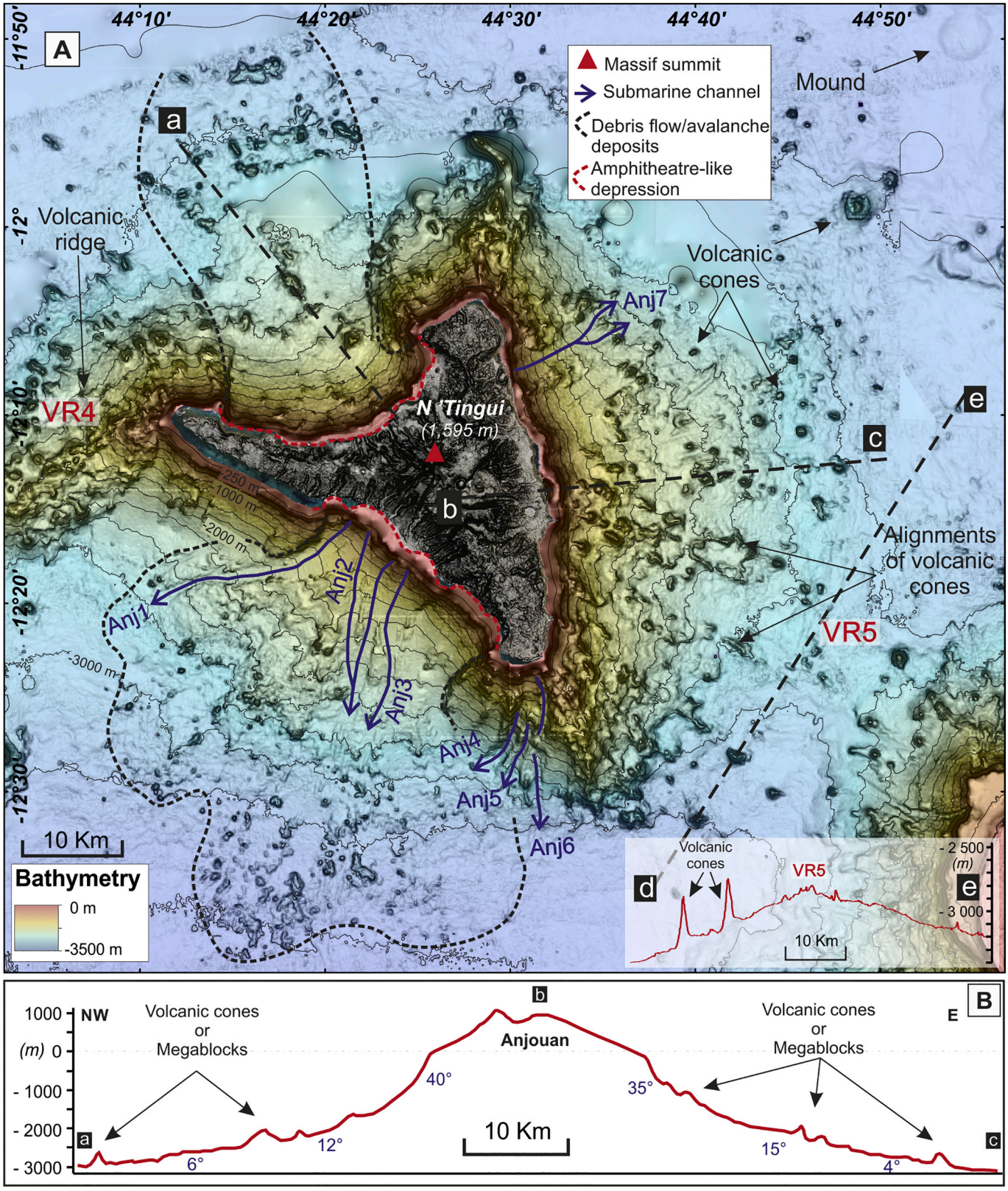

Fig. 4. (A) Morpho-bathymetric map of Anjouan (see location in Fig. 1B). A bathymetric profile (d–e) across the volcanic ridge VR5 is shown. (B) Bathymetric profile (a to c) from NW to E of Anjouan.

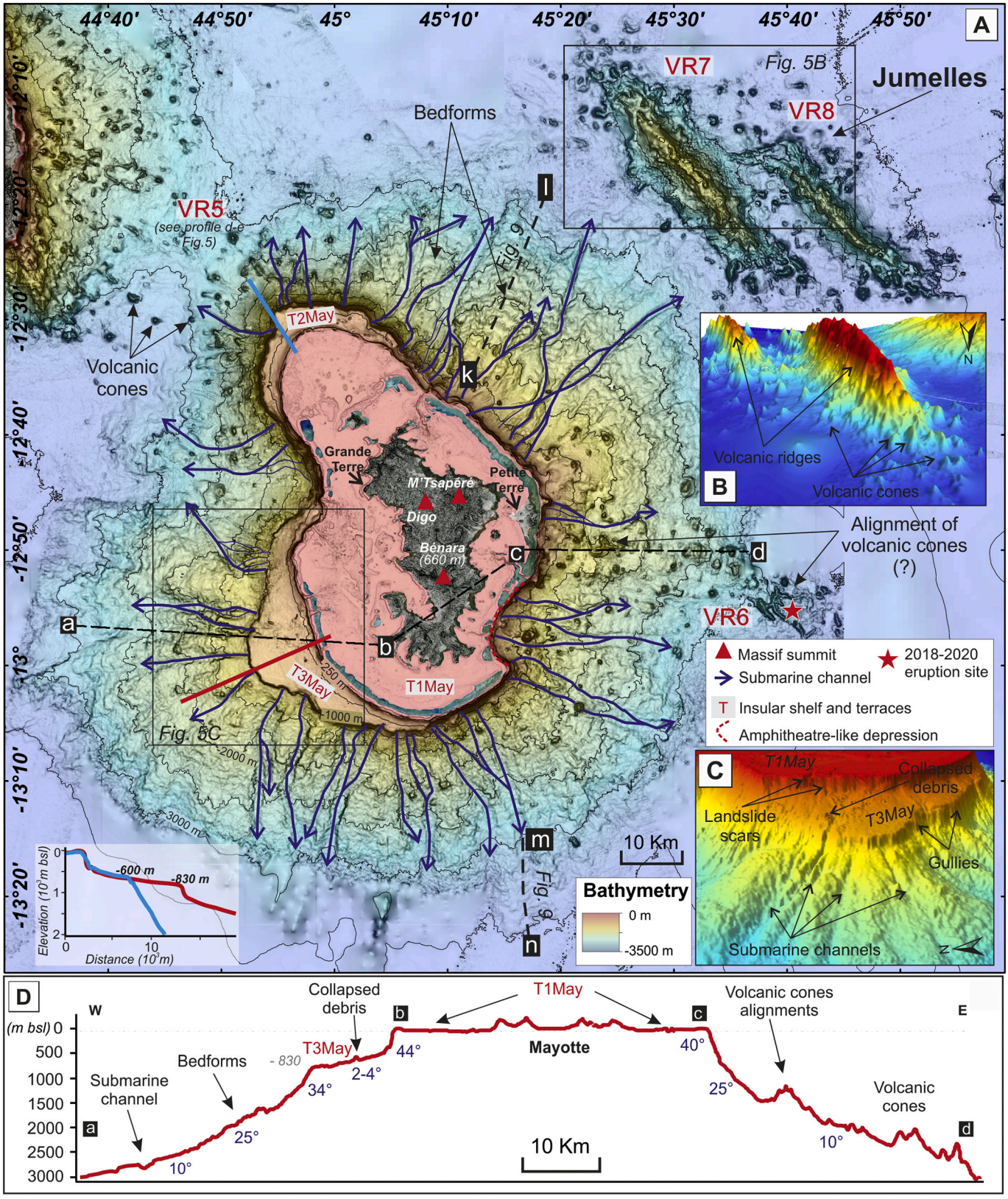

Fig. 5. (A) Morpho-bathymetric map of Mayotte and the Jumelles (see location in Fig. 1B). Two bathymetric profiles intersecting the terraces T2May (in blue) and T3May (in red) are shown. The location of the profiles across the bedform fields shown in Fig. 9 is indicated. (B) Underwater 3D visualization of the Jumelles volcanic ridges. (C) Underwater 3D visualization of the SW terrace T1May. (D) Bathymetric profile (a to d) from W to E of Mayotte. (For interpretation of the references to colour in this figure legend, the reader is referred to the web version of this article.)

3. Material and methods

3.1. Multibeam bathymetry and seismic data

Since 2004, several oceanographic surveys carried out by the French Hydrographic Office (Shom) and the French Geological Survey (BRGM) have enabled the acquisition of data necessary for this study (more than 13,000 km of multibeam bathymetric data and sub-bottom seismic lines, available on data.shom.fr). Five bathymetric Digital Elevation Models (DEMs) at a resolution ranging from 1 m near the shores (<30 m water depths) to 100 m in the deep sea (>30 m to 3500 m water depths) covering the Comoros Archipelago were provided by the Shom. In shallow waters, the bathymetric DEMs are generated through Lidar surveys conducted under the Litto3D® program (Shom – IGN). Multibeam bathymetry data and sub-bottom seismic lines were collected by the Shom essentially on RV *Beautemps-Beaupré* and in the framework of collaborations (e.g. BATHYMAY cruise acquired by BRGM on the R/V *Marion Dufresne*). In addition, external data were also gathered in order to complete the bathymetric coverage of the study area: soundings and isobaths of electronic chart of navigation (ENC) and GEBCO 2014 bathymetric grid. The bathymetric DEMs were subsequently harmonized and gridded into a similar resolution – 100 m - (WGS84 World Mercator) following the method described by Biscara et al. (2016). From this DEM and using ArcGis v10 software, a morpho-bathymetric analysis was performed: geomorphological analysis were made by means of slope, hillshade, 2D and 3D views.

The sub-bottom seismic lines were collected during the Shom 2009–2010 campaigns with a Simrad SBP 120 sediment sounder (CHIRP). It has a modulating acquisition frequency between 2.5 and 7 kHz and provides a maximum vertical resolution of ~20 cm. This makes possible to characterize the acoustic properties of shallow sub-seafloor. Seismic data were processed with The Kingdom © software, two-way travel times (TWT) have been converted in meters using an average seismic velocity of 1500 m.s^{-1}.

3.2. Limits of the study

Data resolution does not allow a precise identification of the morphology of some volcanic and sedimentological features existing all around the Comoros archipelago. Concerning volcanic cones, we are unable to identify reliefs of less than 20 m high. Even for higher landforms, it is sometimes difficult to clearly differentiate volcanic cones from large debris or megablocks. Moreover, the lack of multibeam data in some parts of the archipelago, does not always allow us to accurately characterize the morphologies observed in some submarine portion of the islands, such as the insular shelf, volcanic cones or bedforms.

The lack of both seismic profiles and cores/grab sediment sampler, in order to better understand the internal morphologies and to develop the

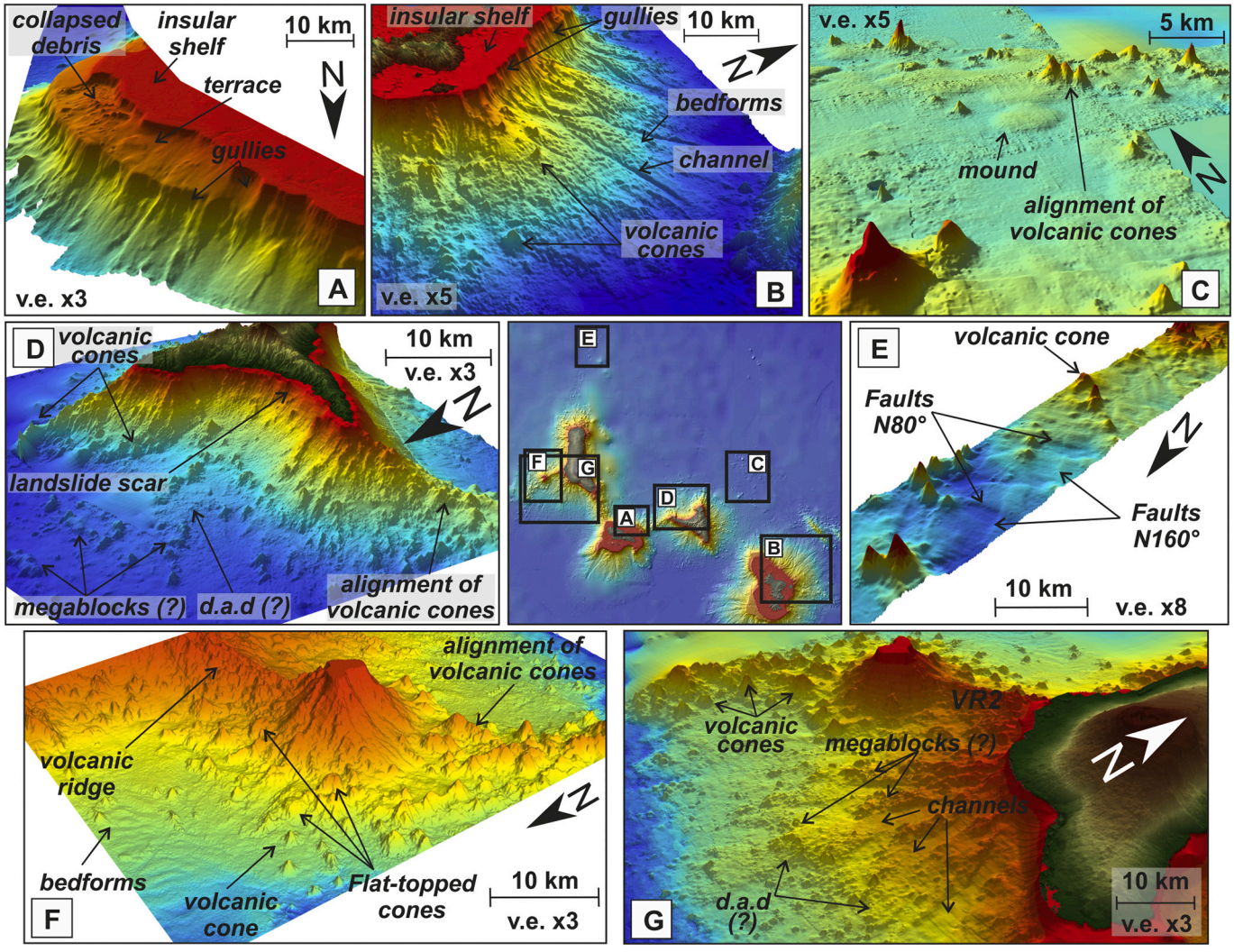

Fig. 6. 3D images showing the main structures recognized throughout the Comoros archipelago. The location of each image is shown in the central map. d.a.d: debris avalanche deposits.

sedimentological and stratigraphic evidences on the shelves and the flanks of the Comoros islands, respectively, prevents further interpretation of the various structures observed from the bathymetric data. The scarcity of previous work, and in particular the lack of geochronological data, often forces us to a merely morphological interpretation. This is for example the case for the terraces. Since those of Mohéli have never been studied, a detailed comparison with those of Mayotte is impossible.

3.3. Terminology

3.3.1. Pointy cones, flat-topped cones, mounds

Volcanic cones and mounds are common features around volcanic

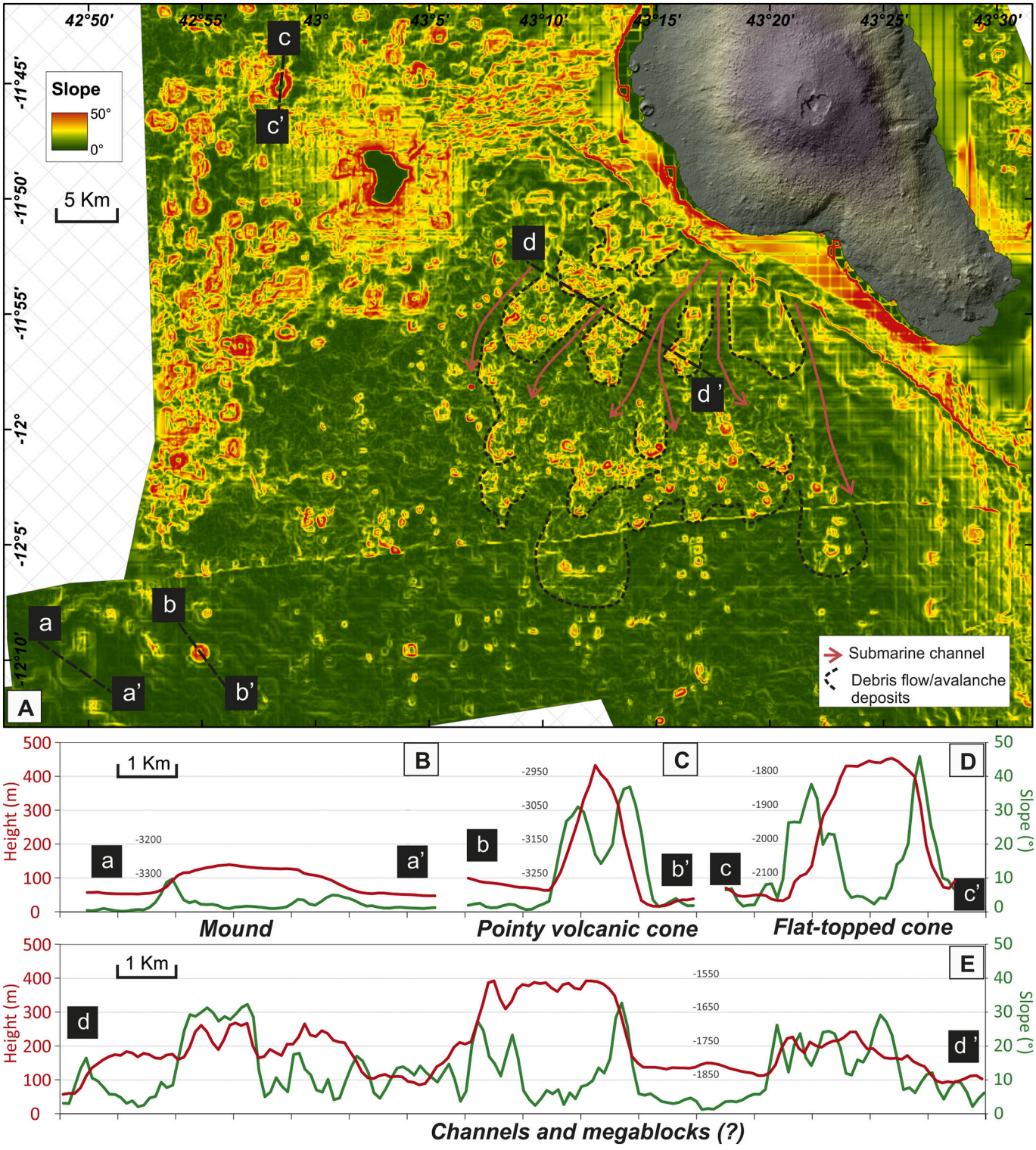

Fig. 7. (A) Slope map of the SW of Grande Comore, and location of the bathymetric profiles (in red) and associated slope gradients (in green) of some selected features: (B) Mound, (C) Pointy volcanic cone, (D) Flat-topped volcanic cone (E) Channels separated by irregular and chaotic surfaces. Several units shaping the area covered by debris avalanche deposits are shown (black dashed lines). (For interpretation of the references to colour in this figure legend, the reader is referred to the web version of this article.)

archipelagoes.

Here, volcanic cones mostly correspond to reliefs with an overall conical "pointy" shape (Figs. 6, 7C). Pointy cones have a base varying from circular to elliptical, and smooth flanks with gradients ranging between 15° and 30°, defined as large hyperbolas on seismic profiles (ET3 on Fig. 8A, B). They are most often isolated (Fig. 6B to G), but can also be aligned and coalescent, constituting alignment of volcanic cones (Fig. 6C to F).

A few flat cones have been identified, mainly at great depths (>1700 m) around Vailheu Bank (Fig. 6F). They have simple, circular to slightly elongated shapes, but their flat and irregular top distinguishes them from pointed cones (Fig. 7D). They have an average basal diameters of 2200 m and an average height of 400 m, smooth flanks with gradients ranging between 30° and 40°.

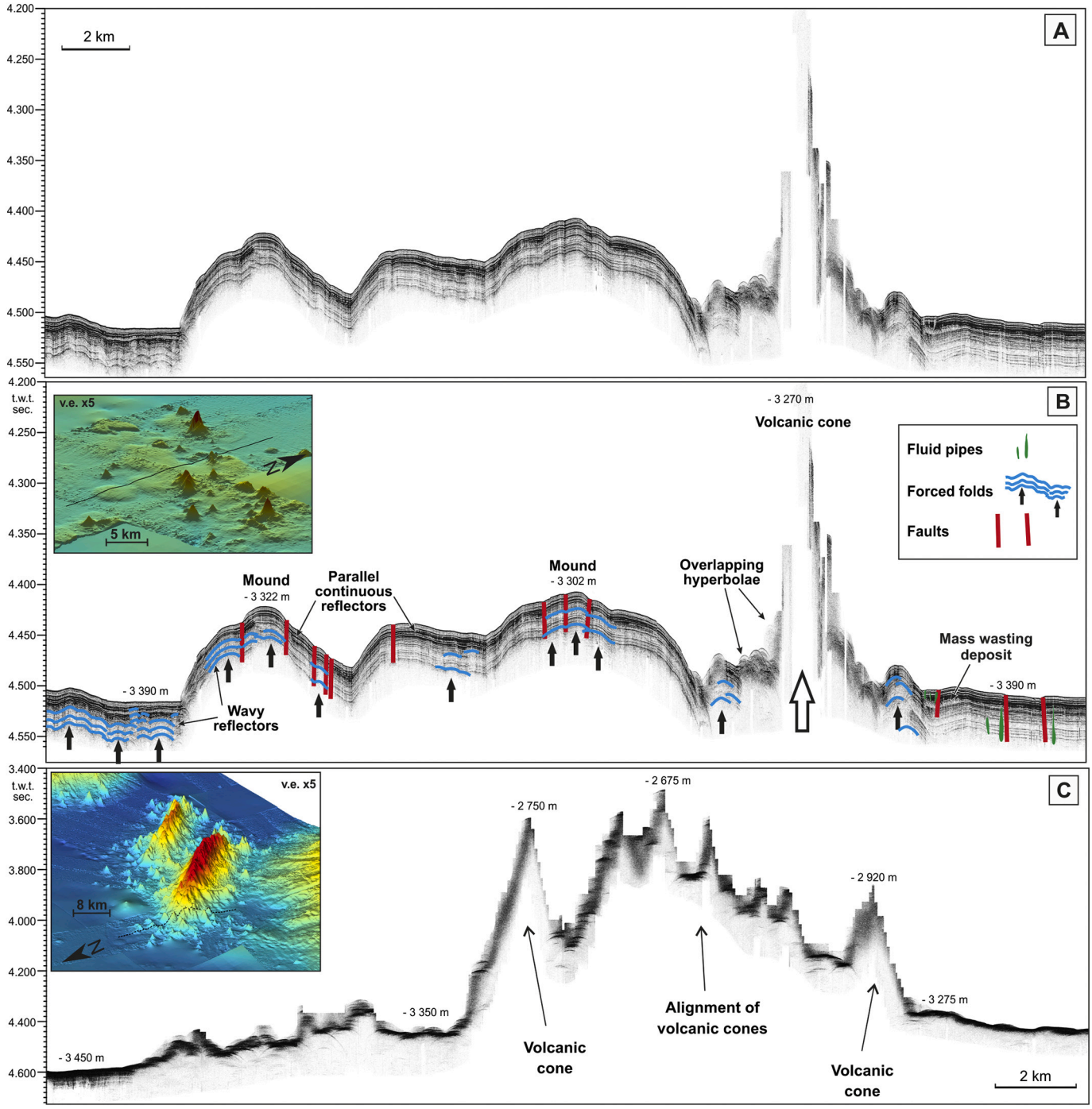

Fig. 8. (A, B) Seismic profiles across volcanic cones and mounds north of the archipelago and southwest of the Jumelles volcanic ridges (see location on Fig. 6C). Different seismic facies have been observed, the most prevalent being a set of parallel, well-stratified reflectors interpreted as sedimentary continuous layers. At some instances, up-bending reflectors are identified on the seafloor and creating large mounds. On the mounds normal faults affect de sedimentary units. At other instances, multiple but no well-defined overlapping hyperbolae, with a low amplitude and chaotic acoustic facies, appear along inclined slopes corresponding to a volcanic cone. At the foot of the cone small chaotic and semitransparent lens can be interpreted as small mass-wasting deposits. Forced folds are present around the volcanic cones and mounds resulting from the extensional and compressional regimes of the area. (C) Seismic profile across the Jumelles volcanic ridge showing an acoustic signature typical of volcanic cones.

Mounds are low relief, sub-circular or sometimes irregular in shape (Figs. 6C, 7B). They show an average surface of 15 km^2 (basal diameter ranging from 2000 to 8500 m) and an average height of 80 m. They are often isolated (as it is the case in the north of the archipelago, Fig. 6C). Small-scale faulting along the summit and the flanks of the mounds and forced folds near the base are visible on the seismic profile (ET2 on Fig. 8A, B).

Other volcanic structures like small volcanic linear ridges or linear fissure eruptions, thick lava flows, are probably present and may be suspected in some places (i.e. east of Mayotte or east of Anjouan). However, the too low resolution of our DEM does not allow defining them precisely. Therefore, they were not taken into account in this study.

3.3.2. Megablocks

The existence of megablocks associated with debris avalanche deposits is strongly suspected. Examples of reliefs with irregular morphology, a few tens to hundred meters high, identifiable as megablocks, are recognizable, for example south of Grande Comore (Fig. 6G) or north of Anjouan (Fig. 6D). However, the too low resolution of the DEM does not allow us to characterize them precisely, and their distinction from volcanic cones is often very tricky. So, it seems unreasonable to us to try to point them out specifically.

3.3.3. Terraces and insular shelves

An insular shelf and two submerged terraces surround Mohéli and Mayotte, as shown on Figs. 3, 5, 6A and B. The presence of these features is an important indicator of sea level changes and/or land subsidence (Quartau et al., 2010; Ramalho et al., 2013). Such features are generally well developed when erosion dominates volcanism. Unfortunately, as explained in Section 3.2, in our case these data cannot be used beyond morphological analyzes.

3.3.4. Channels and gullies

Channels and gullies are shown on Fig. 6A, B and G. Channels surround the islands and may originate in the upper slope, continuing downslope to the basin floor (Fig. 6B, G). In places, gullies are present in the uppermost slopes or mid-slopes, when incision is not deep or narrow enough to form channels (Fig. 6A).

3.3.5. Bedforms

'Wave-like' bedforms are present on the flank of the Comoros Islands (Fig. 6B, F and Fig. 9). They have an average wavelength of 2 km and a wave height ranging between 15 and 130 m according to the islands. They cover at least an area of 4000 km^2, which make them an important feature of the study area. Bedforms correspond to small geomorphic features and are useful for the understanding of the transfer of material from subaerial to deeper marine flanks. Insights are given on the size distribution, the morphology and the genesis of bedforms observed around the submarine volcanic flanks of the islands. These deformed synsedimentary deposits can be generated by gravity instabilities or/and by sediment-laden gravity (Correggiari et al., 2001; Lee et al., 2002; Mulder, 2011; Casalbore et al., 2020).

4. Results

4.1. Grande Comore

Grande Comore's volcanic edifice has an elongated shape, with an N-S orientation (Fig. 1B, 2A). It is extended by three volcanic ridges (VR) characterized by high bathymetry and a high density of volcanic cones, west of Vailheu Bank (VR1), between Grande Comore and Vailheu Bank (VR2), and south of Grande Comore connecting Mohéli (VR3, Fig. 1C). These volcanic ridges are elongated, steep-sided reliefs. Many isolated cones or alignments of volcanic cones are identifiable along the volcanic ridges, and on the submarine flanks of the island. They are present all around the island (average density of 0.3 cone/km^2), but their distribution is not uniform. Two subcircular mounds located in the southwest of the island (average height 40 m, radius 1.5 km) have been identified (Fig. 2A).

West of Grande Comore, the Vailheu Bank is a 9 km^2 submarine terrace exposed occasionally at low tide, with very steep slopes (47 to 50°) near its top (Fig. 2D). Vailheu Bank is located at the extremity of VR2, 20 km west off the coast of Karthala volcano (Fig. 2A and C). The VR2 ridge (N65°) starts close to the west coast of Grande Comore. Its depth increases regularly (mean slope gradient <4°) to reach a water depth of about 1100 m near the base of the Vailheu Bank (Fig. 10A, line 2). The western flank of the Vailheu Bank reaches a depth of 2700 m. Northeast and east of the Vailheu Bank, the submarine slopes gradually decrease without significant escarpment, reaching 1500 m below sea level (bsl). West of the Vailheu Bank, a high density of volcanic cones seems to outline a general N-S to NE-SW oriented alignment (N20°) rising to >1000 m above the surrounding seafloor (VR1). In detail, some alignments of cones seem to be oriented radially with respect to the Vailheu Bank, while others are more or less N-S. Unfortunately, the lack of data west of this ridge does not allow its precise description. The tallest volcanic cone of this study (657 m high) is located about 18 km SW of the Vailheu Bank.

South of Grande Comore, the southeast Karthala rift zone extends offshore up to 13 km from the coast by a topographic ridge about 15 km wide with a gentle slope (~ 4° - Fig. 10A, line 1). It connects to the volcanic ridge VR3 (N160°) located at a mean water depth of 900 m, the deepest part of the ridge being about 1080 m bsl (Figs. 1B, C & 2A). This ridge is connected to Mohéli's edifice with a steep slope (> 30° - Fig. 10A, line 1).

Submarine slopes of Grande Comore are generally steeper than subaerial slopes (Fig. 2D). Areas with rugged morphology and numerous volcanic cones can be distinguished in the submarine morphology, such as, for example, north of La Grille volcano and east of M'Badjini Massif (lines 3 and 5, respectively, on Fig. 10A). In contrast, only few volcanic cones are visible along the southeastern submarine slopes of La Grille Massif, where a smooth morphology is identifiable despite the limited data available in this area. Southwest of Karthala volcano, in a sector bounded by the volcanic ridges VR1/VR2 and VR3, a bathymetric bulge corresponds to a large area of blocky surface morphology (Figs. 2A, 6G, 7A & E). In this area, the mean slope decreases from >30° to <3° from 1000 m to 3000 m bsl (line 1 on Fig. 10B), with less irregularity compared, for example, to the uneven slopes observed north of La Grille Massif. These fan-shaped deposits extend widely on the abyssal plain, to at least 45 km from the coast (Fig. 2A). They are dissected and bound by channels up to 100 m deep (Fig. 7E).

A number of channels, rectilinear in shape, surround submarine slopes of Grande Comore (Fig. 2A). Only one major channel (GC1) has been identified east of the island. CG1 is located northeast of M'Badjini Massif and extends in continuity with one of the major landslide of the eastern flank of Karthala volcano (see Bachèlery and Coudray, 1993). Its southern edge corresponds to the continuation of a scarp identified on land. The widest channel (GC2) is located in the southern part of the island and is 46 km long and 3 km wide, originating from a spectacular landslide amphitheater affecting the southern flank of Karthala. Other significant channels, around 20 km long and 2 km wide, can be identified around Grande Comore (Fig. 2A): mainly to the southwest (GC3, GC4 and GC5), separated by interfluves with irregular blocky surfaces, and north (GC6, GC7, GC8) separated by interfluves that may represent preserved portions of the submarine flanks, formed through alignments of volcanic cones and possibly the superimposition of lava flows and other volcanic products (Fig. 2B). Channels are also present north and west of the Vailheu Bank but are smaller in size (3 to 11 km long and 1 km wide).

Bedforms are present, especially on the northwestern submarine flanks (profile 'd-e' in Fig. 2A, Fig. 6F, Fig. 9). The range of bedforms wavelengths and wave heights is 1 to 2.7 km and 25 to 45 m,

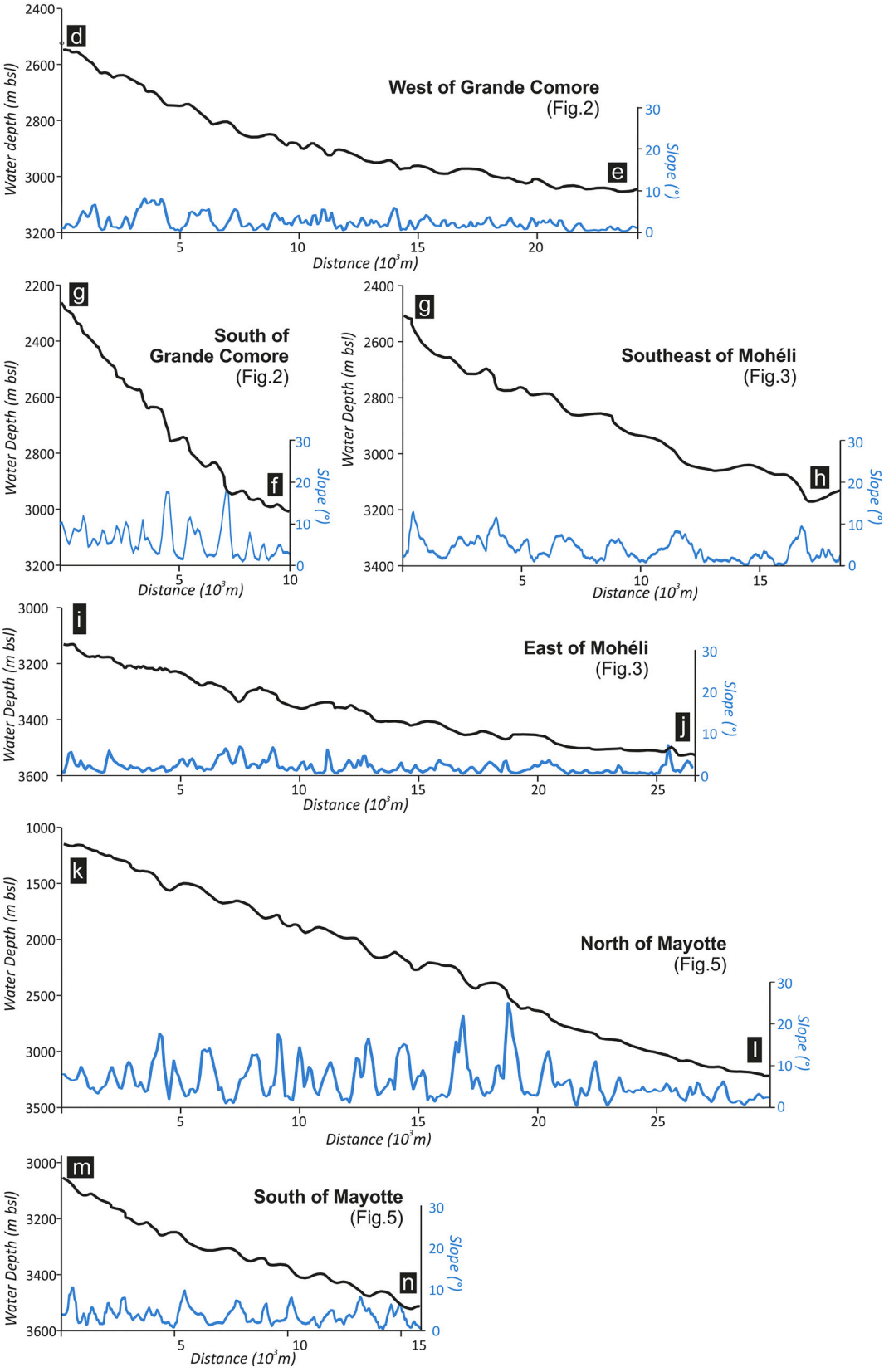

Fig. 9. Bathymetric profiles (in black) and slope gradients (in blue) along the profiles of some bedform fields identified off Grande Comore (profiles' location in Fig. 2), Mohéli (profiles' location in Fig. 3) and Mayotte (profiles' location in Fig. 5). (For interpretation of the references to colour in this figure legend, the reader is referred to the web version of this article.)

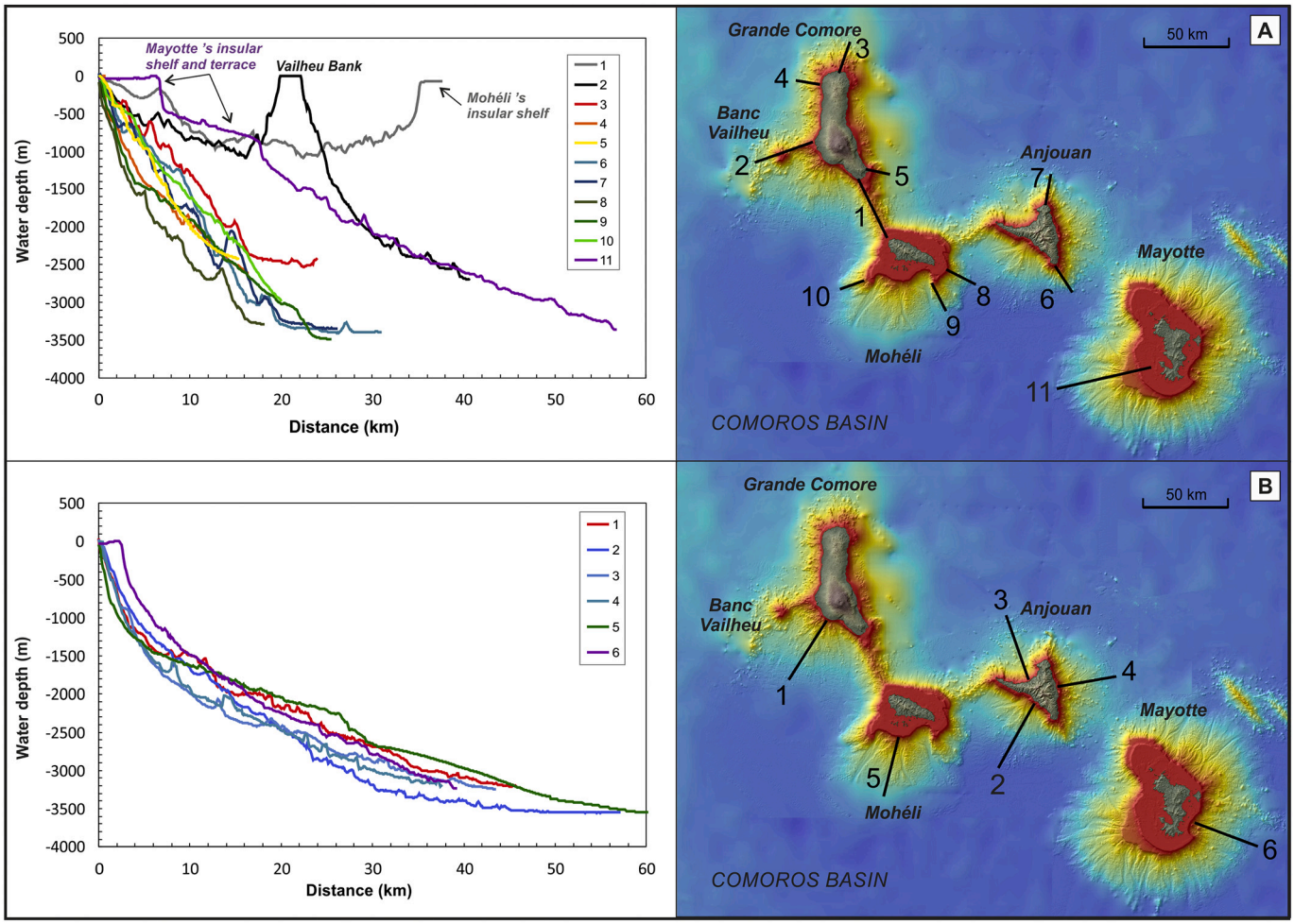

Fig. 10. (A) Bathymetric profiles along submarine constructional volcanic flanks off the Comorian Islands. Flanks show rectilinear shaped slopes characterized by many irregularities mainly corresponding to volcanic cones. In comparison to the other Islands, Mayotte has gentler slopes reflecting a significant spreading of the formations and a higher sediment cover. (B) Bathymetric profiles along flanks affected by landsliding. All profiles have an overall concave upwards shape. The slightly convex zone downslope may result from debris avalanche deposits accumulation. Vertical exaggeration is ~7:1. Profile locations and lengths are shown on the corresponding map on the right.

respectively, for a slope gradient of 2.5° (slope gradients varying in average between 8.3° and 0.3° - Fig. 9). No clear evolution of the bedform morphologies is observed through depth. However, bedforms are also identified south of Grande Comore and perpendicular to VR3 (profile 'g-f' in Fig. 2A, Fig. 9). Between 2600 and 2900 m bsl, bedforms are significant with a maximum wavelength and height of 1.1 km and 50 m, respectively, and highest slopes of 17° (Fig. 9). Their size decreases below 2900 m: respectively, 0.7 km and 10 m and an average slope of 6°.

Grande Comore seems to have a single, little developed insular shelf with an edge located around 100 m water depth. Unfortunately, bathymetric data are missing at shallow depth, which unable the possibility for further descriptions of the insular shelf.

4.2. Mohéli

Mohéli is located at the junction of two elongated volcanic ridges, VR3 already described, originating from Grande Comore, and VR4, at an average depth of 1700 m, connecting Mohéli and Anjouan (Figs. 1D, 3A). The orientation of VR4 (N55°) is almost parallel to VR2 connecting Grande Comore to the Vailheu Bank (N65°). Volcanic cones are identifiable on the two volcanic ridges VR3 and VR4 (Fig. 3C). Mohéli's volcanic edifice has an approximately rectangular shape, with two large amphitheaters affecting its southern flank. The flanks east, southeast and southwest of Mohéli (respectively lines 8, 9 and 10 on Fig. 10A) are irregular, with slope gradients mainly ranging from 14° to 5°. They are incised by small channels (8 to 10 km long, ~1 km wide). The density of volcanic cones appears to be low (around 0.1 volcanic cones per km^2). Several large volcanic cones can be identified on the rugged terrain east of Mohéli (Fig. 3A and line 8 in Fig. 10A), in line with the general orientation of the island and following the alignment of the most recent cones recognized ashore. This may be the offshore extension of the old Mohéli volcanic rift zone.

While the northern and western submarine flanks of Mohéli are characterized by very steep and smooth upper slope surfaces, two huge amphitheater-like depressions that open downslope, and a fan-shaped bathymetric bulge with chaotic terrains, characterize the area south of Mohéli (Fig. 3A). In this area, networks of tributary channels coalesce to form three large channeled systems (Mo1, Mo2, Mo3). Mo1 is the largest channel of 60 km long and 2 km wide. These channels have interfluves shaped by the chaotic terrains, on which we can identify bedforms and volcanic cones and/or megablocks (Fig. 3A, D). Unfortunately, multibeam data are missing south of Mohéli to fully describe this southern flank. Available data show bedforms reaching 3500 m depth, more than 70 km from the island. Bedform in the southeast of Mohéli (profile 'g-h' in Fig. 3A and Fig. 9) have wavelengths and wave heights ranging from 1.3 to 2.2 km and 50 to 80 m, respectively. Slope gradient varies from 12.5° to 0.1°, with an average value of 4°. Between 2700 and 2800 m bsl,

the bedform wavelength is higher than in the deeper section of the flank. In the eastern flank of Mohéli, south VR4, bedforms are located at a water depth ranging from 3130 and 3500 m (profile 'i-j' in Fig. 3A and Fig. 9). The range of bedform wavelengths and wave heights is, respectively, 1.2 to 2.2 km and 15 to 55 m (average slope gradient 2°, Fig. 9). The highest average slope gradient is 7° and the lowest 0.1°, but no clear evolution of the morphologies is observed through depth.

An insular shelf and two submarine terraces developed around Mohéli. The insular shelf T1Moh is large with a broadly rectangular shape and a surface area of 987 km^2, and a shelf break located at 0–100 m bsl (Fig. 3A). The submarine terraces T2Moh, to the southwest of Mohéli, and T3Moh, to the northeast and east, are located at ~600 m bsl (Fig. 3A), with a surface area of 52 km^2 and 112 km^2, respectively. Numerous small landslide scars affect T1Moh (Fig. 3B). The slopes that connect T1Moh to T2Moh and T3Moh vary from 25 to 40°. From the edge of T1Moh, the slope is very steep, dipping up to 45°, then decreasing offshore to a depth of 2500 m in the north and 1500–2000 m in the south (profile 'a-b' on Fig. 3D).

4.3. Anjouan

The three peninsulas shaping the island of Anjouan extend underwater with rugged slopes (Fig. 4). The south volcanic rift zone (N152°) extends more than 18 km offshore towards the south, while the northern peninsula shows a submarine extension of 16 km. The submarine extension of the western peninsula forms a 90° angle, with respect to the orientation of the subaerial part, to connect Mohéli by a volcanic ridge (VR4 - Fig. 4A). Many volcanic cones are identifiable along and near these ridges. East of the island, isolated volcanic cones and volcanic cone alignments are more densely concentrated on the middle part of the eastern flank. This corresponds to a positive morphology (more than 1000 m above the surrounding seafloor) between Anjouan and Mayotte (Fig. 1E and profile 'd-e' in Fig. 4A). It suggests the existence of a submarine ridge of NW-SE orientation towards Mayotte (VR5 - N130°). Some structures in this area form small linear ridges visible over several kilometers. Given the resolution of our DEM, it is difficult to interpret it (see Section 3.3). The density of cones is estimated between 0.1 and 0.3 volcanic cones per km^2 according to the area.

The northern and southwestern flanks show broad embayments, and steep and smooth concave upper slopes. On the lower slopes, an area with irregular blocky topography extends over several tens of kilometers (Fig. 4A, B, Fig. 6D). Large channels have formed, with three major channels (Anj1, Anj2 and Anj3) located on the southwestern flank, (16 to 23 km long and 1 to 2 km wide). Northeast and south of Anjouan, smaller channels (10 km long and 1.5 km wide) have also developed (Anj4, 5, 6 and 7 - Fig. 4A).

Anjouan has a single, little developed insular shelf, with steep upper slopes from the shelf break (40° on the northwest and southwest of the island and 35° in the east) gradually decreasing downslope (4°) reaching a depth of 3000 m (Fig. 4A, B).

4.4. Mayotte

The submarine morphology of Mayotte reflects the onland geological framework of the island with a NW-SE elongation for the northern part of the island, and a semi-circular morphology in the south (Fig. 5A). Volcanic cones are scattered around Mayotte. Their density is low (max 0.1 volcanic cones per km^2), except for two areas in the northwest of the island towards Anjouan (VR5, previously described), and towards the east where a WNW-ESE oriented volcanic ridge (N120°, VR6), extending from the recent volcanism of Petite Terre to about 3500 m bsl, is clearly visible (0.2 cones per km^2). This ridge is the site of the current seismicity and ongoing volcanic eruption (Fig. 5). One of the tallest volcanic cones in the study area (520 m high) is located on this ridge, close to the current eruptive center that is more than 800 m high (Feuillet et al., 2019).

On the western and southern flanks of the island, the submarine slopes show a slightly concave shape and a chaotic surface with many undulations (Fig. 5A, D). Submarine channels are homogeneously present on all of the flanks, from the base of the reef plateau to the base of the edifice. These channels are radial to Mayotte but their morphology is mostly sinusoidal (see Audru et al., 2006 for more details - Fig. 5A). A fan-shaped field is formed by a series of channels and interfluves. Between the channels, bedforms were recognized all around the island and are present between 1500 and 2700 m bsl (Fig. 6B). The range of bedforms wavelengths and wave heights is 1 to 2 km and 40 to 130 m, respectively (profile 'k-l' in Fig. 5A and Fig. 9). They are crescentic and the average slope gradient is 6°. The largest bedforms occur between 2150 and 2700 m bsl. Bedforms also occur in the bed of the channels (profile 'm-n' in Fig. 5 and Fig. 9) with a range of wavelengths and wave heights of 1 to 1,7 km and 25 to 40 m, respectively. They are crescentic downslope and have an average slope gradient of the bedforms is 3.5° (Fig. 9). At 3250 m of water depth, bedforms are more pronounced with a slope gradient up to 10°.

An insular shelf and two submarine terraces have been previously identified (see Audru et al., 2006). Mayotte's insular shelf T1May is the largest of the Comoros archipelago (1860 km^2). A lagoon has been formed with an almost continuous reef barrier, and with the insular shelf edge located at 0–50 m water depths. Channels and karst systems (150 m bsl) are visible on the insular shelf (Audru et al., 2006 – Fig. 5). Two small terraces (Fig. 5A) are located in the northwest of Mayotte (T2May) at 450–600 m bsl (area of 123 km^2), and in the southwest of Mayotte (T3May) at a depth varying from 450 to 830 m bsl (area of 291 km^2). Each terrace is delimited on its upper and lower edges by steep slopes, and its top slopes gently down (2–4° - Fig. 5D and line 11 in Fig. 10A). Several landslide scars affect the terrace T1May (Fig. 5C). This is particularly obvious in the southeast where T1May shows a clear amphitheater-shaped landslide scar, with concave slopes lower down (Fig. 5A and line 6 on Fig. 10B). On the terraces T2May and T3May, collapsed debris deposits can be observed (Fig. 5C, D). The slopes that connect T1May to T2May and T3May vary from 40 to 45°, decreasing offshore with slightly concave gentle slopes (5°).

4.5. The Jumelles ridges

Northeast of Mayotte, two NW-SE (N140°) parallel submarine ridges (VR7 and VR8), named the Jumelles, form isolated reliefs elevating as much as 2160 m above the seafloor (Table 1, Fig. 1B, F). The Jumelles correspond to elongated landforms, with relatively rough slopes, and numerous volcanic cones and alignments of volcanic cones (Figs. 5B, 8C). The density of volcanic cones is high with 0.2 cones per km^2. One of the tallest volcanic cones of this study (538 m high) is located south of the Jumelles.The two ridges differ in size and elevation. The western ridge (VR7) is 46 km long, 15 km wide and 2200 m high, whereas the eastern one (VR8) is 35 km long, 10 km wide and 1500 m high. No submarine channels or chaotic terrains are present. At the northern end of VR8, a group of volcanic cones seems to be aligned along an ENE-WSW orientation (N70°), close to that found for the ridges VR2 (between Karthala and Vailheu Bank) or VR4 (Anjouan and Mohéli). This alignment appears to extend across VR7 (Fig. 5A).

5. Discussion

5.1. Submarine volcanism

Detailed bathymetric mapping makes it possible to immediately identify two types of morphologies rising over an abyssal plain at depth locally exceeding 3500 m (Fig. 1B, F): (1) central volcanoes forming islands and their submarine bedrock, and (2) elongated volcanic ridges, more or less prominent above the abyssal plain, interconnecting, or not, these islands (Fig. 1 and Table1). This is a major morphological character of the Comoros archipelago.

Table 1
Morphologic characteristics of the main landforms of the Comoros archipelago.

	Type	Edifice height (m)	Lower depth (m bsl)	Higher altitude (m) or depth (m bsl)	Number of submarine terraces
Grande Comore	Volcanic island	5543	3182	2360	1
Vailheu	Bank	2796	2800	4 bsl	1
Mohéli	Volcanic island	4338	3548	790	3
Anjouan	Volcanic island	4867	3272	1595	–
Mayotte	Volcanic island	4164	3504	660	3
Jumelles	Volcanic ridges	2160	3400	1240 bsl	–

5.1.1. *Overall morphology of the submarine volcanic islands' flanks*

As for many other volcanic islands (e.g. Gee et al., 2001; Mitchell et al., 2002; Mitchell, 2003; Geist et al., 2006; Masson et al., 2002, 2008; Chiocci et al., 2013), the submarine flanks of the Comorian Islands show constructional volcanic areas and slopes that have undergone erosive-depositional processes. Volcanic constructional flanks (Mitchell et al., 2002) are recognized from their rough and uneven morphology, due to the presence of numerous volcanic cones, eruptive fissures and lava flows. They are interpreted as directly built by volcanic eruptions, even if they may have undergone later erosion and sedimentation. The presence of numerous volcanic cones and alignments of volcanic cones characterizes the constructional submarine flanks of the Comoros Islands. Data resolution does not allow clear identification of lava flows, even if lobate outlines are sometimes identifiable. For Grande Comore, Anjouan and Mohéli, average slope gradients of the constructional flanks are almost steady (about 8° to 10°) or slightly decreasing downslope (lines 3 to 10 on Fig. 10A). In comparison to the other Comorian Islands, Mayotte's submarine slopes are gentler (~ 5° - line 11 on Fig. 10A) and smoother, reflecting a significant spreading of the formations building the submarine flanks of this island and a higher sediment cover. Sediments are largely covering Mayotte's submarine flanks, while few volcanic cones are identifiable, except for the northwest (VR5) and the east (VR6) of the island (Fig. 5A).

Compared to constructional ones, flanks affected by landslides show smoother surfaces and have slope profiles showing a clear gradual decrease in slope gradient, passing from steep upper slopes (>40°) to downslope moderate (3–10°) gradients (Fig. 10B). For some of them, the profile changes in the mid-slope from concave to locally slightly convex, likely determined by deposit accumulation (lines 1, 3, 5 on Fig. 10B). Landslide scars at the insular shelf edges and coastlines can be frequently identified upslope these flanks. The general morphology of the deposit accumulations, sometimes defining a fan-shaped bulge with blocky and hummocky surface morphology, allows us to interpret these deposits as debris avalanche deposits. Such flank morphologies, the general shape of the deposits and the occurrence of upslope landslides scars, allow to infer that these morphologies are likely related to large-scale failure events. They are similar to what has been described for many other volcanic islands (e.g., Canary Islands, Ablay and Hürlimann, 2000; Masson et al., 2002; Acosta et al., 2003; Mitchell et al., 2002; Hunt et al., 2014; Cape Verde, Masson et al., 2008; Aeolian Islands, Romagnoli et al., 2009, 2013; Hawaiian Islands, Moore et al., 1989; Moore et al., 1994; Morgan et al., 2003; La Reunion Island, Oehler et al., 2008; Le Friant et al., 2011).

5.1.2. *Volcanic rift zones*

The existence of volcanic rift zones characterizes the subaerial part of the Comorian shield volcanoes (Bachèlery et al., 2016; Famin et al., 2020). Volcanic rift zones are preferential pathways that transport magma from a shallow magma reservoir to the flank of the volcano. They are caused by internal and gravitational stresses (e.g. Dieterich, 1988; Tilling and Dvorak, 1993). In Grande Comore, the volcanic rift zones are well defined by alignments of cinder and spatter cones along eruptive fissures. They form a typical ridge-like topography (Bachèlery et al., 2016). The shape of Anjouan is clearly reminiscent of the youngest Canary Islands El Hierro, Tenerife and La Palma, with wide coastal embayments and a three-armed geometry corresponding to volcanic rift zones. Such an association, with triple 'Mercedes Star' rift zones and giant lateral collapses affecting the flanks of these rift zones, reveals a growth of the volcanic edifice controlled by active volcanism (Carracedo, 1994, 1996).

With the exception of the SE rift zone of Karthala (Fig. 2), which extends to a depth of about 1000 m, with an average slope of ~4° before connecting with VR3 (line 1 on Fig. 10A), and possibly the rift zones of Anjouan, the submarine slopes do not show any significant offshore extension of the volcanic rift zones recognized on land. This is for example the case for the volcanic rift zones north of the Karthala and Grille massifs (Fig. 2A).

In the Comoros Islands, submarine flanks built by repeated intrusive/eruptive activity (constructional flanks) form areas, extending up to ~20 km from the coast, whose morphologies range from *short linear ridges*, as the SE rift zone of Karthala volcano and the S rift zone of Anjouan, to a broader *"fan-like"* geometry, as for the constructional flanks of Mohéli and the northern submarine flanks of La Grille Massif and Anjouan. The Comoros Islands do not have well-developed rift zones as those around Hawaiian Islands, spreading up to 50 km from the coast. Actually, they have similarities with those observed in La Réunion Island (Lénat et al., 2012), the Galapagos Islands (Geist et al., 2006) or the Canary Islands (Gee et al., 2001; Mitchell et al., 2002; Acosta et al., 2003). Such morphologies suppose a reduced capacity for magma to laterally intrude into the rift zones, from underlying magma chambers. Acosta et al. (2003) have already discussed this difference in morphology for the Canary Islands. The main similarities between Comoros and Canary archipelagoes lie in the chemical composition of the magmas (both alkaline, versus more tholeiitic magmas for the Hawaiian shields), a low magma production rate, a more complex history of volcano building, a slow absolute plate motion, and a lesser depth of the sea floor around the islands and consequently, a lesser elevation of the islands above it. This influences the gravitational stress field on volcanic edifices and the ability of magma to propagate into rift zones.

5.1.3. *Submarine volcanic ridges*

Eight major volcanic ridges have been identified from the bathymetric data (VR1 to 8). They are elongated, steep-sided reliefs, with numerous volcanic cones and alignments of volcanic cones. Their volcanic origin can be deduced from the acoustic texture and the morpho-bathymetric analyses revealing their uneven morphology and, for some of them, the youthfulness of remarkably preserved reliefs. The aligned distribution of the volcanic cones and orientation of the volcanic ridges suggest that they are built along lithospheric fault system (Muffler et al., 2011). Three of the volcanic ridges are located between the main islands of the archipelago (between Grande Comore and Mohéli - VR3, between Mohéli and Anjouan - VR4, and between Anjouan and Mayotte - VR5) (Fig. 1C, D, E). Furthermore, VR2 connects Grande Comore to the old volcanic edifice of Vailheu Bank (Figs. 1, 2 and line 2 on Fig. 10A). This indicates strong interaction between active tectonic and volcanic processes (Duffield et al., 1980; Bacon, 1982; Connor and Conway, 2000; Valentine and Krogh, 2006; Gaffney et al., 2007).

The average depth of these volcanic ridges increases from Grande Comore to Mayotte (Fig. 1F). Between Anjouan and Mayotte, the ridge VR5 is less discernible but we suggest its existence, based on a clearly

positive morphology (see profile 'd-e' in Fig. 4) and the higher density of cones. The fact that this ridge is less visible could be explained by an older age of volcanic activity and a partial blanketing by sedimentary cover. The volcanic ridge VR6 (site of the ongoing eruption – Fig. 5) spreads from the eastern flank of Mayotte. Cones, eruptive fissure ridges, lava flows and plateaus, mounds, and inflated lava flow have been recognized along and near this volcanic ridge (Paquet et al., 2019).

Without collected samples, we can only postulate that the volcanic activity on the volcanic ridges of the Comoros archipelago is probably mainly related to mafic magmatism along active lithospheric fissure systems, as indicated by the prevalence of pointy morphology of the volcanic cones and their frequent alignment, as observed for other oceanic volcanic islands (e.g. Casalbore et al., 2015; Clague et al., 2019). However, more evolved compositions (intermediate and silicic magmas) may have been locally responsible of eruptions, as evidenced by the variability of composition of the magmas dredged on the ridge east of Mayotte (VR6), and the evolved compositions of the magmas feeding the 2018–2020 eruption off Mayotte (Bachèlery et al., 2019; (Berthod et al., n.d). These volcanic ridges can be considered as 'monogenetic volcanic fields', resulting from multiple episodic eruptions building monogenetic volcanoes (see Smith and Németh, 2017; Németh and Kereszturi, 2015). If so, this implies the genesis of magma batches below the volcanic ridges in discrete fusion events with a defined chemical composition (Smith and Németh, 2017). Their distribution provides evidence of the existence of lithospheric fractures allowing episodic access for deep magmas. However, we are aware that high-resolution studies of the Comorian submarine volcanic ridges need to be carried out in order to verify their origin.

5.1.4. Volcanic cones and mounds

A large number of volcanic cones crop out offshore the Comoros Islands. They are found at all depths, even if about 70% of them are located at more than 2000 m bsl. Volcanic cones are mostly present on the submarine flanks of the islands and on the volcanic ridges, but also isolated on the abyssal plain, sometimes at more than 70 km from the nearest island (Fig. 6C, F).

Some 1650 volcanic cones have been measured on the surveyed area. The morphological parameters (regular shape, conical to elliptical, size and aspect ratio) are those classically encountered for submarine cones around volcanic islands or ridges (Clague et al., 2000; Romero Ruiz et al., 2000; Mitchell et al., 2012; Casalbore et al., 2015; Romagnoli et al., 2020). Some morphometric parameters of the volcanic cones encountered in the Comoros archipelago are shown in Fig. 11. These values are similar to those obtained for the submarine pointed cones of the Azores (Stretch et al., 2006; Mitchell et al., 2012; Casalbore et al., 2015; Weiß et al., 2015), or Linosa, Sicily Channel (Romagnoli et al., 2020) and a bit different from those in Canary (Mitchell et al., 2002; Romero Ruiz et al., 2000) and Hawaii (Clague et al., 2000; Wanless et al., 2006) with values around 0.08 (Fig. 11). The highest volcanic cones (over 300 m in height) have a slightly higher than average aspect ratio (0.21 vs. 0.15), reflecting smaller diameter with respect to the cone height. This suggests that they develop preferentially upwards rather than outwards. As shown by the 'Cône Elianne', a 700 m high volcanic cone on the southern flank of Piton de la Fournaise volcano, La Réunion (Saint-Ange et al., 2013; Michon, 2016) or by the more than two-years-long ongoing eruption located on the volcanic ridge (VR6) off the eastern coast of Mayotte (Feuillet et al., 2019), the significant size of the Comorian submarine pointed cones (120 m in average, and up to 820 m high for the Mayotte ongoing eruption) may be related to a long duration of eruption and the high initial volatile content of the alkalic magmas emitted along the archipelago. It is difficult to infer eruptive regimes based only on the analysis of bathymetric data. Many parameters are involved, such as water depth, magma discharge rate and composition, including volatile content. The eruption of chemically homogeneous, undegassed, volatile-rich, magma may favor formation of pointed cones (Clague et al., 2000; Wanless et al., 2006).

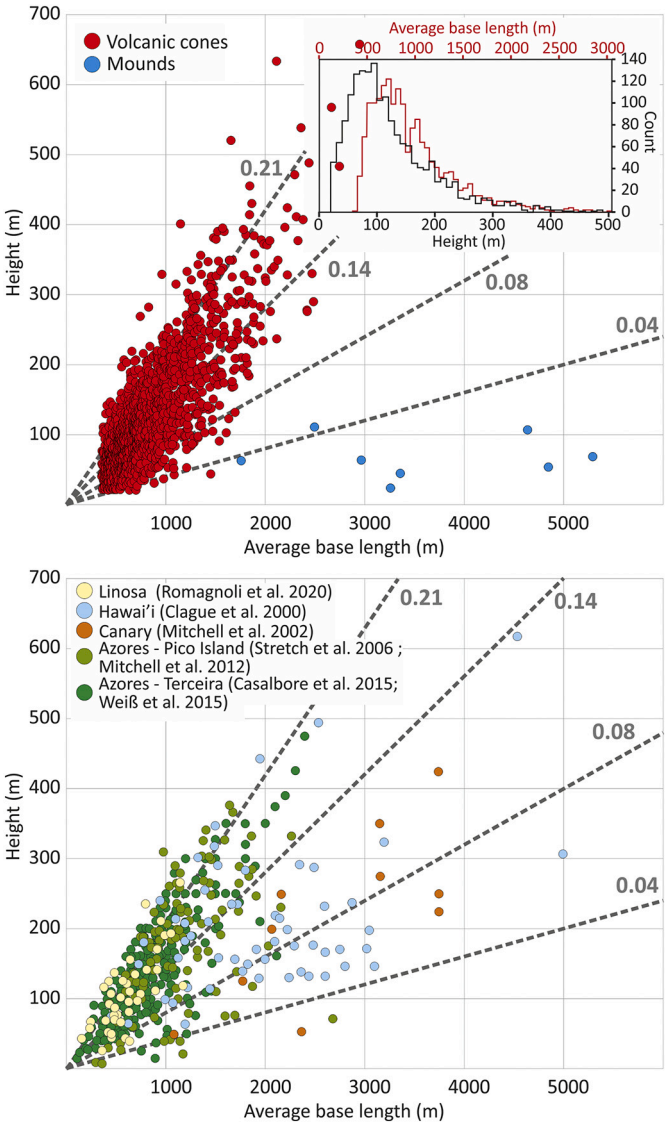

Fig. 11. Characteristics of the volcanic cones and mounds around the Comoros archipelago (upper graph). Basal diameter vs. height of volcanic cones and mounds; dashed lines indicate values of aspect ratio (height/diameter). The measured volcanic cones have basal diameters ranging from 300 to ~3000 m, and an average height of 120 m. Sixty-five large cones have heights greater than 300 m (15 are over 400 m high). Their aspect ratio is 0.15 in average, with a slightly higher aspect ratio (0.21) for the highest (over 300 m) volcanic cones. Mounds mostly have aspect ratios lower than 0.04, with basal diameter up to 5000 m and heights not exceeding 120 m. In the lower graph, volcanic cones for other volcanic islands are shown for comparison. The volcanic cones surrounding the Comorian Islands have great similarities with those observed in the Azores.

Around the Comoros Islands, rare flat-topped cones (Figs. 6F, 7D) have been observed, always at great depths. They are considered as the result of long-lived steady effusive eruption of magma of low viscosity and volatile content, at low to moderate effusion rate, on low slopes (Clague et al., 2000; Wanless et al., 2006).

Several mounds have been recognized throughout the Comoros archipelago, on the abyssal plain or next to volcanic ridges (Fig. 12), in areas where a sedimentary cover allows their injection: SW of Grande Comore (Fig. 2A, C) and NE of Anjouan (Figs. 4A, Fig. 6C). Compared to volcanic cones, their aspect ratio (H/W) is very low (<0.04) (Fig. 7B, 11). Mounds are considered as surface expressions of flat magmatic intrusive bodies (sill-type intrusions) emplaced at shallow structural

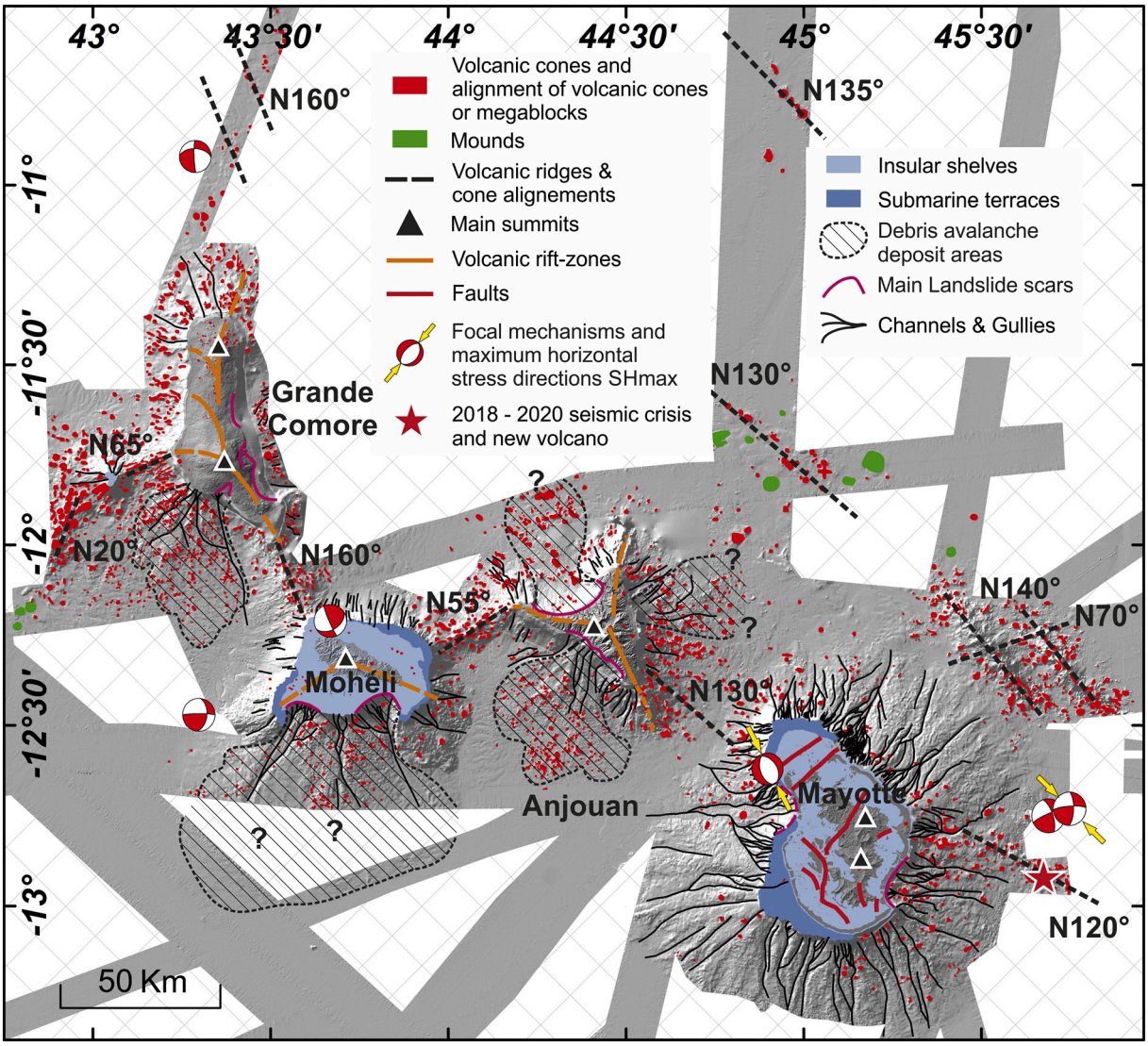

Fig. 12. Synthesis map of the main structures recognized throughout the Comoros archipelago. The main structural, volcanic and sedimentary features identified throughout our morpho-bathymetric study are shown here, as well as data from the literature such as volcanic rift zones and landslide scars on land (Bachèlery et al., 2016; Famin et al., 2020), fractures affecting the island and the insular shelf of Mayotte (Audru et al., 2006) and focal mechanisms (CMT 1976–2017, Lemoine et al., 2020).

level and related to hydrothermal–volcanic activity (Medialdea et al., 2017; Sanchez-Guillamón et al., 2018). Magma injection causes differential uplifting, forced folding and faulting of the overlying sedimentary layers, and can induce the transport of hot fluids to the surface. According to the morphostructural classification of Sanchez-Guillamón et al. (2018) based on the Canary Basin, the Comorian mound morphologies are similar to the subcircular mounds corresponding to the morphostructural type 2 (group A), in good agreement with a sill-like intrusion into the sedimentary cover (Sanchez-Guillamón et al., 2018). We identify small-scale faulting along the summit and the flanks of the mounds (Fig. 8A, B), which can be interpreted as vertical fracture pipes and hence fluid migration pathways, and forced folds near the base that may result from the elevation generated by the intrusive bodies (Sanchez-Guillamón et al., 2018). However, lower-resolution seismic profiles or multichannel profiles are needed to better characterize the magmatic activity and to image the internal structure of the mounds, to confirm the presence of sill intrusions and the location of hydrothermal vent complexes, as well as their age.

5.2. *Erosive-depositional processes*

Unfortunately, no information is available on the age of the mass-wasting events, but the presence of bedforms, scars and debris avalanche deposits indicate very active mass-wasting processes on the submarine portions of the Comorian islands.

5.2.1. *Large-scale and small-scale instabilities*

Large-scale failure events have been identified from flank morphology, the existence of hummocky terrains interpreted as debris avalanche deposits and the occurrence of upslope horseshoe-shaped scars (see *5.1.1 Overall morphology of the submarine volcanic islands' flanks*). Large-scale flank instability events may radically change the topographic profile of the affected area and this change remains perceptible even if subsequent events occur (Masson et al., 2002). Landslide scars at the insular shelf edge are common features observed along the submarine flanks of insular volcanoes (Casalbore et al., 2014, Chiocci and Casalbore, 2017; Ricchi et al., 2020).

Well-defined amphitheater-shaped structures that could correspond to landslide's scars are easily identified southwest of the Karthala Massif,

south of Mohéli, north and south of Anjouan and southeast of Mayotte (respectively Figs. 2, 3, 4 and 5). Fan-shaped bulges and hummocky terrains, interpreted as debris avalanche deposits, cover the submarine flanks downslope the landslide scars (Fig. 6D, G). Slope gradient maps allow to better evidence units suggesting that the submarine bulges have formed by the emplacement of multiple mass-wasting deposits (Fig. 7A). We assume that the hummocky surface morphology of the debris avalanche deposits is shaped by a large number of blocks. However, the resolution of the bathymetry does not allow to finely characterize these hummocky surfaces. As previously mentioned, we cannot surely identify megablocks, and it would be unreasonable to try to distinguish them from volcanic cones that could have been built after the debris avalanche deposition. Data with a higher resolution need to be acquired to better characterize these deposits and to verify the existence of volcanic cones built a posteriori. It is also crucial to determine the age of the deposits and their exact meaning in the evolution of the islands.

Southeast of Karthala volcano, the amphitheater-shaped structure is small (Fig. 2A), irrelevant with respect to the extension of the debris avalanche deposits observed on the submarine flank of this volcano. This implies that the volcanic activity in this area lasted long enough after the debris avalanche deposit, to build a convex coastline and cover most of the landslide scar associated with these deposits. The overall morphology is quite different for the flank landslides identified in Mohéli, Anjouan and Mayotte, for which landslide scars are clearly identifiable, implying reduced volcanic activity after the collapse. In Mayotte, a large amphitheater-like scar is visible cutting across the southeastern edge of the insular shelf (affecting T1May). However, we cannot identify associated debris avalanche deposits. Except for the submarine volcanic ridge at the east of the island (VR 6), the submarine flanks of Mayotte have smooth and gentle slopes with many small slope failures and channels. The spreading of volcaniclastic products appears to be wider than for the other islands of the archipelago (Fig. 10A), probably related to the greater age of Mayotte volcanism, and thus the prevalence of gravitational processes of erosion/deposition over a longer period of time.

Collapsed debris, related to small-scale mass-wasting events, are observed on the outer edge of the insular shelves of Mohéli (Figs. 3B, 6A) and Mayotte (Fig. 5C), similarly to that observed in the Aeolian Islands of Lipari, Stromboli and Vulcano (Casalbore et al., 2011; Romagnoli et al., 2013; Casalbore et al., 2016). Most recent landslides are identified by the presence of collapsed debris deposits on the terraces T2May and T3May (Fig. 5A, C, D). Some of the debris deposits are large in size reaching 0.5 km^2 and can be associated with landslide scars affecting the insular shelf edge, the terraces and the upper slopes.

5.2.2. Gravity flows processes and associate submarine landforms

Submarine channel systems are developed diversely depending on the islands, indicating evolutionary differences. Some islands are surrounded by well-developed submarine canyon-channel systems (i.e. Mayotte), while others are characterized by younger and little developed channel systems (i.e Grande Comore) (Fig. 12). We consider that the younger islands tend to have a high volcanic activity and a poorly developed hydrographic system both in the mainland and the submarine section, as it is the case for Grande Comore. On the contrary, numerous channels drain oldest volcanic islands' submarine flanks, while a very low density of cones is present, such as for Mayotte.

The development of channels may be related to the overall shape of the volcanic edifice. The submarine channels around the islands mainly have a straight morphology resulting from the steepness of the uppermost and mid-slopes of the islands (Clark et al., 1992). However, as the slopes decrease (around 20°), gullies and channels converge and gradationally merge downslope into a single channel (Mo1 and Mo3 in Mohéli, Anj2 and Anj7 in Anjouan, and the majority of Mayotte's channels), while in some cases, channels bifurcate and split into multiple channels (GC3 and GC4 in Grande Comore). Around Mayotte, the extensive incision of gullies and channels in the submarine flanks and their sinusoidal shape confirm the maturity of its channelized system. The channels' heads mostly affect the outer edge of the insular shelf/marine terraces (Fig. 5C) and their formation likely started at the time these terraces were emerged (as proposed by Audru et al., 2006) during low-stands of the relative sea level.

On the upper steep slopes of the volcanic edifices (> 20°), no bedforms are formed but gullies or/and channels incise the flanks of the islands. The sediment-laden flows erode the seafloor impeding the formation of small-scale bedforms (Schlager and Camber, 1986; Micallef and Mountjoy, 2011; Clare et al., 2018). In higher water depths ranging from 1400 m to 3500 m and when flanks gradients decrease (<20°), large-scale bedforms occur throughout the archipelago, with a range of wavelengths and wave heights being respectively, 1 to 2,7 km and 15 to 80 m (Fig. 9). Where the channelized system is well developed, large-scale bedforms, with an average wavelength of 1.5 km are sometimes present between the channels, as it is the case for Mohéli and Mayotte (Figs. 3, 5). Bedforms are also present inside the channels of Mohéli and Mayotte, but are smaller in size than those in the interfluve (Fig. 9). According to Cartigny et al. (2011), bedforms in the interfluves correspond to potential overspilling locations, assuming that bedforms form perpendicular to the flows. Gravity flows or unconfined turbidity currents might be at the origin of the bedforms, and the frequent change in the gradient slope of the bedforms as seen in Fig. 9, the result of the changes in flow thickness, velocity and specific discharge (e.g. Wynn et al., 2002; Cartigny et al., 2011; Postma and Cartigny, 2014). The development of volcaniclastic turbidite systems is associated with these large-scale bedforms, result of unconfined gravity flows mainly supplied from riverine input (Mazuel et al., 2016), which correspond to the Comoros case. The same morphologies have been reported in Stromboli and Panarea Islands (Sicily) and La Réunion Island (Mazuel et al., 2016; Casalbore et al., 2020). Also, the southern flank of Mohéli clearly reminds the northern flank of Porto Santo of the Madeira archipelago (Casalbore et al., 2020), where bedforms located in the flanks of the islands are associated to the arcuate headwall scars, resulting from gravity flows originated by seafloor displacements.

5.3. Relative chronology of the volcanism

The chronology of the volcanism along the Comoros archipelago is still an open question. Mayotte's morphology, with its wide shelf and well-developed fringing reef, contrasts with that of the little eroded and active shield volcanoes in Grande Comore. This suggests a rejuvenation of volcanism from east to west. Nevertheless, the ongoing eruption 50 km east of Mayotte is disrupting this pattern (Fig. 12). Some considerations and a relative chronology of the volcanism can be deduced from geomorphological features, erosion stages, the presence or absence of a developed insular shelf and terraces, the overall shape and gradient of slopes, the more or less developed channelized systems and the abundance of volcanic cones (Fig. 12).

Grande Comore and Anjouan are high altitude volcanic islands with only very narrow shelves and no submarine terraces visible today. Pristine volcanic morphologies, with numerous volcanic cones, eruptive fissures and lava flows, are clearly identifiable on Grande Comore (Bachèlery et al., 2016), while ash cones are well preserved and little affected by erosion on Anjouan (Nougier et al., 1986; Famin et al., 2020), enabling volcanic rift zones to be identified for these two islands (Fig. 12). In contrast, Mohéli and Mayotte are lower islands characterized by a well-developed insular shelf, as well as ancient terraces located between 450 and 600 m bsl for Mohéli (T2Moh and T3Moh) and between 450 and 830 m bsl for Mayotte (T2May and T3May).

Terraces are considered as paleo-sea level markers (Casalbore et al., 2017; Ricchi et al., 2018). We have no information about the nature and age of the Mohéli terraces. Concerning Mayotte, the channels and karst systems on the insular shelf would have been formed at the end of the last glacial maximum (20 to 18 kyr), when the lagoon and the reef emerged (Dullo et al., 1998; Audru et al., 2006; Montaggioni and

Martin-Garin, 2020). For Audru et al. (2006), the two terraces of Mayotte, now underwater, would have also formed in the subaerial domain, as shown by the presence of erosion channels on their surface. They propose that they were formed during the Pliocene (2.6 Ma and 3.9 Ma for T2May and T3May, respectively), based on their average depth, and considering a steady subsidence rate of 0.19 mm/year. Even considering a higher subsidence rate (0.25 mm/year, Camoin et al., 1997; Montaggioni and Martin-Garin, 2020), this indicates that, on Mayotte, erosion dominates over volcanism during the last million years. Wider shelves, like those of Mohéli and Mayotte, are commonly associated with older volcanic centers (Romagnoli et al., 2018). The strong indentations of the coastline or insular edge also confirm the advanced stage of these islands. Although little is known about the terraces of Mayotte and Mohéli, the common features regarding their insular shelves and terraces (depth, size) argue in favor of a similar origin and age, and seem to indicate a common geological history of these two islands. The presence of terraces at great depths provides evidence of subsidence that has affected the islands of Mayotte and Mohéli, but without independent age control, it is not possible to decipher the relative effects of sea level fluctuations and active subsidence of the volcanic substratum.

The Grande Comore volcanoes show a typical shield volcano morphology little modified by erosion, similar to the volcanoes of Big Island – Hawaii. Many volcanic cones are visible on the submarine slopes of Grande Comore, in accordance with the young age of this edifice and its frequently active volcanism. The morphology of Anjouan also shows strong similarities with that of volcanic islands with recent volcanic activity, by its modeled embayments and its triple-armed geometry rift zones, which indicate, according to MacDonald (1972), active rift zones (see Section 5.1.2*Volcanic rift zones*). Primary volcanic morphologies (volcanic cones, alignments of volcanic cones) are also particularly well preserved on the submarine flanks of the islands of Grande Comore and Anjouan, compared to Mohéli and Mayotte. Volcanic cones appear less numerous and less easily identifiable on the smoother submarine flanks of these islands. In addition, eroded volcanic bedrock, submarine flanks with multiple slope breaks and gentle slopes obscured by a significant sedimentation and widespread volcaniclastic deposits, surround Mayotte. Finally, the channelized system around Anjouan is less developed compared to Mohéli, while around Mayotte the channels are prevalent on the whole submarine flanks.

The morphological considerations listed above indicate that, if Mayotte is indeed the oldest of the islands of the Comorian archipelago, Mohéli is significantly older than Anjouan. Anjouan could therefore be the second youngest island in the archipelago after Grande Comore. The available geochronological data seem to suggest that Mohéli would be younger than Anjouan. But the paucity of geochronological data, and the fact that all dated rocks belong to the subaerial domain, explain this discrepancy with our conclusions. Thus, the progression of ages along the Comorian archipelago must be reconsidered.

Michon (2016) propose that volcanic activity in Mohéli and Anjouan began 7 to 10 Ma ago, about 10 Ma later than in Mayotte. As the oldest islands appear to be Mayotte and Mohéli, we can assume that volcanism migrated northward from these volcanic centers, to extend to Anjouan and later to Grande Comore. The formation of the volcanic ridges of the Jumelles on the seafloor in the east of Mayotte, seems to be recent, as shown by the morphological freshness of these ridges, the high density of volcanic cones, and the paucity of sediment coverage (Fig. 8C). In the same way, the current eruption in the east of Mayotte Island (Feuillet et al., 2019) is a magnificent illustration of the possibilities of resuming activity after several millennia of rest. This clearly demonstrates that, throughout the archipelago, volcanism can resume at any time.

5.4. Structural control on volcanism

One of the outstanding features of volcanism in the Comoros Archipelago is the existence of submarine volcanic ridges interconnecting the main islands (Figs. 1 and 12). This unique pattern, with a close association of main central volcanoes at different stages of evolution, like those of Grande Comore, Mohéli, Anjouan and Mayotte, and volcanic ridges composed of the juxtaposition of many monogenetic volcanic edifices, highlights a strong link between regional tectonics and magmatism. Linear volcanic ridges can be considered as the result of magma emplacement into a pre-existing damaged lithosphere (Neves et al., 2013). They can be seen as the surface expression of a monogenetic magmatism controlled by lithospheric extension along the ridge axis, which, for the Comoros archipelago, could correspond to the diffuse plate boundary between the Somali Plate and the Lwandle Plate, as proposed by Famin et al. (2020). Indeed, in areas close to volcanic ridges, such as west of Grande Comore or east of Mohéli, bedforms probably emanating from compressional zones occur, due to a morphological expression of thrust.

Two main sets of tectonic orientations (Fig. 12) are highlighted by the distribution of volcanic ridges, but also by the directions of volcanic rift zones and small-scale elongated volcanic features such as alignments of cones and faults (Fig. 6C, F). The first group corresponds to structures ranging from N120° to N160°, with the volcanic ridges VR2, VR5, VR6, VR7 and VR8, the rift zones SE of Karthala volcano and SE of Anjouan, and alignments of cones (e.g. NE of Anjouan and N of Grande Comore). A second group is composed of globally oriented WSW-ENE ridges, with the volcanic ridges VR1 and VR3, and alignments of cones (e.g. north of VR8 and across VR7). These orientations are coherent with regional extensional and trans-tensional fault systems as reported by Deville et al. (2018) for the southern part of the Mozambique Channel, or normal fault escarpments observed along the Sakalaves Seamounts by Courgeon et al. (2018). Available focal mechanisms near the Comoros Islands (Fig. 12) indicate normal faulting and strike slip, with an orientation compatible to a NE-SW tensional axis (Lemoine et al., 2020). Thus, the revelation of volcanic ridges along the seafloor of the Comoros archipelago is consistent with the interpretation of the Comoros archipelago as a dextral shear zone potentially being the northern boundary of the Lwandle plate, as proposed by Famin et al., 2020. As for Canary Islands (Geyer and Martí, 2010), the origin and evolution of the volcanic islands of the Comorian archipelago are strongly controlled by regional tectonic structure. In such a context, the main volcanic islands constituting the Comoros archipelago have grown over the main loci of genesis and magma transfer, whereas a more diffuse volcanism occur along the volcanic ridges.

6. Conclusions

The morpho-bathymetric analysis of the Comoros archipelago allowed us to discover the shape and geomorphology of each island's submarine flanks, from their insular shelf to the abyssal plain. The Comorian volcanic edifices include both active volcanic edifices and volcanic islands with well-developed carbonated insular shelves (up to 10 km wide from the coast to the insular shelf edge) and terraces located at depth of more than 400 m. Despite the geographical location of the islands, geomorphological analyses (e.g. erosion stages, presence or absence of a developed insular shelf and terraces, overall shape and gradient of slopes of the submarine flanks, more or less developed channelized systems) clearly show that Mayotte and Mohéli Islands are on top older edifices compared to Anjouan and Grande Comore. We propose a new relative chronology concerning the Comorian volcanism, the youngest to the oldest islands being respectively, Grande Comore, Anjouan, Mohéli and Mayotte. Large-scale instabilities and debris avalanche deposits, gravity flows processes and large-scale bedforms, channelized system maturity and density of volcanic cones and mounds have also been described.

One of the major volcanological and structural features of Comorian volcanism is the close coexistence of central volcanoes forming islands, with elongated volcanic ridges interconnecting, or not, these islands. The existence of submarine volcanic ridges interconnecting the central

volcanoes highlights the close link between regional tectonics and magmatism. The magmatic feeding of the Comoros archipelago seem to occur with, on the one hand, a strong magmatic supply focused under one or several main volcanoes at different stages of evolution, and on the other hand, a magmatism located along elongated volcanic ridges, controlled by lithospheric extension and composed of monogenetic edifices. The orientation of the volcanic ridges coincides to the regional faulted structures interpreted as the seaward prolongation of the East African Rift and those of Madagascar. The Comorian volcanism seem to be strongly connected with the regional lithospheric fractures, induced by the Somalian/Lwandle plates boundary and/or the Karoo rifting episodes. The genesis of the Comoros archipelago is most probably linked to lithospheric deformations, rather than the unique result of a deep mantle plume motion.

Declaration of Competing Interest

The authors declare that they have no known competing financial interests or personal relationships that could have appeared to influence the work reported in this paper.

Acknowledgments

The authors would like to thank the technical and scientific shipboard parties of the R/V *Marion Dufresne* (BATHYMAY cruise), the Shom (French Hydrographic Office) and the BRGM (French Geological Survey) for the high resolution data acquired with multibeam echosounders, but also for Lidar surveys conducted under the Litto3D® program by the Shom. An additional thank to the technical and scientific shipboard parties of the BHO *Beautemps-Beaupré* for the acquisition of high resolution seismic profiles (CHIRP). Finally, we would like to thank the five reviewers, including Daniele Casalbore, Laurent Michon, Claudia Romagnoli and Luis Somoza, without their expertise and constructive comments, this paper could not have taken its complete and structured form. This is a LabEx Clervolc contribution n° 446.

References

Ablay, G.J., Hürlimann, M., 2000. Evolution of the north flank of Tenerife by recurrent giant landslides. J. Volcanol. Geotherm. Res. 103, 135–159. https://doi.org/10.1016/S0377-0273(00)00220-1.

Acosta, J., Uchupi, E., Smith, D., Muñoz, A., Herranz, P., Palomo, C., Llanes, P., Ballesteros, M., ZEE Working Group, 2003. Comparison of volcanic rifts on La Palma and El Hierro, Canary Islands and the Island of Hawaii. Mar. Geophys. Res. 24, 59–90. https://doi.org/10.1007/s11001-004-1162-6.

Audru, J.-C., Guennoc, P., Thinon, I., Abellard, O., 2006. Bathymay: la structure sous-marine de Mayotte révélée par l'imagerie multifaisceaux. Compt. Rendus Geosci. 338, 1240–1249. https://doi.org/10.1016/j.crte.2006.07.010.

Bachèlery, P., Coudray, J., 1993. Carte volcano-tectonique (1/50000e) de la Grande Comore et notice explicative. In: Coopération MFdl (Ed.), Carte Géologique des Comores. Ministère Français de la Coopération.

Bachèlery, P., Villeneuve, N., 2013. Hotspots and large igneous provinces. In: Shroder, J., Owen, L.A. (Eds.), Treatise on Geomorphology, Tectonic Geomorphology, 5. Academic Press, San Diego, CA, pp. 193–233.

Bachèlery, P., Ben Ali, D., Desgrolard, F., Toutain, J.P., Coudray, J., Cheminee, J.L., Delmond, J.C., Klein, J.L., 1995. L'éruption phréatique du Karthala (Grande Comore) en juillet 1991. Comp. Rendus Acad. Sci. Paris 320 (II–a), 691–698.

Bachèlery, P., Morin, J., Villeneuve, N., Soulé, H., Nassor, H., Radadi Ali, H., 2016. Structure and eruptive history of Karthala volcano. In: Bachèlery, Patrick, Lénat, Jean-François, Di Muro, Andrea, Michon, Laurent (Eds.), Active Volcanoes of the Southwest Indian Ocean. Springer Berlin Heidelberg, Berlin, Heidelberg, pp. 333–344. https://doi.org/10.1007/978-3-642-31395-0_22.

Bachèlery, P., Berthod, C., Di Muro, A., Gurioli, L., Besson, P., Caron, B., Deplus, C., 2019. Petrological and Geochemical Characterization of the Lava From the 2018-2019 Mayotte Eruption: First Results. AGU, Fall Meeting San Francisco, V52D-06.

Bacon, C.R., 1982. Time-predictqble bimodal volcanism in the Coso Range. Calif. Geol. 10, 65–69.

Berthod, C., Médard, E., Bachèlery, P., Gurioli, L., Di Muro, A., Peltier, A., Komorowski, J-C., Benbakkar, M., Devidal, J-L., Langlade, J., Besson, P., Boudon, G., Rose-Koga, E., Deplus, C., Le Friant, A., Bickert, M., Nowak, S., Thinon, I., Burckel, P., Hidalgo, S., Kaliwoda, M., Jorry, S., Fouquet, Y., Feuillet, N. The 2018-ongoing Mayotte submarine eruption: magma migration imaged by petrological monitoring. Earth Planet. Sci. Lett., submitted.

Binard, N., Hekinian, R., Stoffers, P., 1992. Morphostructural study and type of volcanism of submarine volcanoes over the Pitcairn hot spot in the South Pacific. Tectonophysics 206 (1992), 245–264. https://doi.org/10.1016/0040-1951(92)90379-K.

Biscara, L., Maspataud, A., Schmitt, T., 2016. Coastal risk assessment: Generation of bathymetric digital elevation models along French coasts. Hydro Int. (September 2016), 26–29. http://www.hydro-international.com/content/article/coastal-risk-assessment.

Bourhane, A., Comte, J.-C., Join, J.-L., Ibrahim, K., 2016. Groundwater prospection in grande comore island—joint contribution of geophysical methods, hydrogeological time-series analysis and groundwater modelling. In: Bachèlery, P., Lenat, J.-F., Di Muro, A., Michon, L. (Eds.), Active Volcanoes of the Southwest Indian Ocean. Springer Berlin Heidelberg, Berlin, Heidelberg, pp. 385–401. https://doi.org/10.1007/978-3-642-31395-0_24.

Camoin, G.F., Davies, P.J. (Eds.), 1998. Reefs and Carbonate Platforms in the Pacific and Indian Oceans, Special Publication Number 25 of the International Association of Sedimentologists. Blackwell Science, Oxford; Malden, MA, USA.

Camoin, G.F., Montaggioni, L.F., Braithwaite, C.J.R., 2004. Late glacial to post glacial sea levels in the western Indian ocean. Mar. Geol. 206, 119–146.

Carracedo, J.C., 1994. The Canary Islands: an example of structural control on the growth of large oceanic-island volcanoes. J. Volcanol. Geotherm. Res. 60 (3–4), 225–241.

Carracedo, J.C., 1996. Morphological and structural evolution of the western Canary Islands: hotspot-induced three-armed rifts or regional tectonic trends? J. Volcanol. Geotherm. Res. 72, 151–162.

Cartigny, M.J.B., Postma, G., van den Berg, J.H., Mastbergen, D.R., 2011. A comparative study of sediment waves and cyclic steps based on geometries, internal structures and numerical modeling. Mar. Geol. 280 (2011), 40–56. https://doi.org/10.1016/j.margeo.2010.11.006.

Casalbore, D., Bosman, A., Romagnoli, C., Chiocci, F.L., 2014. Submarine mass-movements on volcanic islands: examples from the Aeolian Archipelago (Italy). In: Lollino, G. (Ed.), Engineering Geology for Society and Territory, 4. Springer International Publishing, pp. 199–203.

Casalbore, D., 2018. Volcanic islands and seamounts. In: Submarine Geomorphology. Springer, Cham, pp. 333–347.

Casalbore, D., Romagnoli, C., Bosman, A., Chiocci, F.L., 2011. Potential tsunamigenic landslides at Stromboli Volcano (Italy): insight from marine DEM analysis. Geomorphology 126 (2011), 42–50.

Casalbore, D., Romagnoli, C., Pimentel, A., Quartau, R., Casas, D., Ercilla, G., Hipólito, A., Sposato, A., Chiocci, F.L., 2015. Volcanic, tectonic and mass-wasting processes offshore Terceira Island (Azores) revealed by high-resolution seafloor mapping. Bull. Volcanol. 77 (2015), 24. https://doi.org/10.1007/s00445-015-0905-3.

Casalbore, D., Bosman, A., Romagnoli, C., Di Filippo, M., Chiocci, F.L., 2016. Morphology of Lipari offshore (Southern Tyrrhenian Sea). J. Maps 12 (1), 77–86. https://doi.org/10.1080/17445647.2014.980858.

Casalbore, D., Clare, M.A., Pope, E.L., Quartau, R., Bosman, A., Chiocci, F.L., Romagnoli, C., Santos, R., 2020. Bedforms on the submarine flanks of insular volcanoes: new insights gained from high-resolution seafloor surveys. Sedimentology 2020. https://doi.org/10.1111/sed.12725.

Cesca, S., Letort, J., Razafindrakoto, H.N.T., Heimann, S., Rivalta, E., Isken, M.P., Nikkhoo, M., Passarelli, L., Petersen, G.M., Cotton, F., Dahm, T., 2020. Drainage of a deep magma reservoir near Mayotte inferred from seismicity and deformation. Nat. Geosci. 13, 87–93.

Chiocci, F.L., Casalbore, D., 2017. Unexpected fast rate of morphological evolution of geologically-active continental margins during Quaternary: examples from selected areas in the Italian seas. Mar. Pet. Geol. 82, 154–162. https://doi.org/10.1016/j.marpetgeo.2017.01.025.

Chiocci, F.L., Romagnoli, C., Casalbore, D., Sposato, A., Martorelli, E., Alonso, B., Estrada, F., 2013. Bathy-morphological setting of Terceira Island (Azores) after the FAIVI cruise. J. Maps 9 (4), 590–595.

Chorowicz, J., 2005. The East African Rift System. J. Afr. Earth Sci. 43 (1–3), 379–410. https://doi.org/10.1016/j.jafrearsci.2005.07.019.

Clague, D.A., Moore, J.G., Reynolds, J.R., 2000. Formation of submarine flat-topped volcanic cones in Hawai'i, Research article. Bull. Volcanol. 62 (2000), 214–233.

Clague, D.A., Paduan, J.B., Caress, D.W., Moyer, C.L., Glazer, B.T., Yoerger, D.R., 2019. Structure of Lō'ihi Seamount, Hawai'i and Lava flow morphology from high-resolution mapping. Front. Earth Sci. 7, 58. https://doi.org/10.3389/feart.2019.00058.

Clare, M.A., Le Bas, T., Price, D.M., Hunt, J.E., Sear, D., Cartigny, M.J.B., Vellinga, A., Symons, W., Firth, C., Cronin, S., 2018. Complex and cascading triggering of submarine landslides and turbidity currents at Mvolcanic Islands revealed from mintegration of high-resolution onshore and offshore surveys. Front. Earth Sci. 6, 223.

Clark, J.D., Kenyon, N.H., Pickering, K.T., 1992. Quantitative analysis of the geometry of submarine channels: implications for the classification of submarine fans. Geology 20, 633–636.

Class, C., Goldstein, S.L., Altherr, R., Bachèlery, P., 1998. The process of plume–lithosphere interactions in the ocean basins—the case of Grande Comore. J. Petrol. 39 (5), 881–903.

Coffin, M.F., Rabinowitz, P.D., 1987. Reconstruction of Madagascar and Africa: evidence from the Davie fracture zone and western Somali basin. J. Geophys. Res. Solid Earth Planets 92 (B9), 9385–9406. https://doi.org/10.1029/JB092iB09p09385.

Connor, C.B., Conway, F.M., 2000. Basaltic volcanic fields. In: Sigurdsson, H. (Ed.), Encyclopedia of Volcanoes. Academic Press, San Diego, California, pp. 331–343.

Coombs, M.L., Clague, D.A., Moore, G.F., Cousens, B.L., 2004. The growth and collapse of Waianae volcano, Hawaii, as revealed by exploration of its submarine flanks. Geochem. Geophys. Geosyst. 5 (8) https://doi.org/10.1029/2004GC000717.

Correggiari, A., Trincardi, F., Langone, L., Roveri, M., 2001. Styles of failure in heavily sedimented highstand prodelta wedges on the Adriatic shelf. J. Sediment. Res. 71, 218–236.

Counts, J.W., Jorry, S.J., Leroux, E., Miramontes, E., Jouet, G., 2018. Sedimentation adjacent to atolls and volcano-cored carbonate platforms in the Mozambique Channel (SW Indian Ocean). Mar. Geol. 404, 41–59.

Courgeon, S., Bachèlery, P., Jouet, G., Jorry, S.J., Bou, E., BouDagher-Fadel, M.K., Révillon, S., Camoin, G., Poli, E., 2018. The offshore east African rift system: new insights from the Sakalaves seamounts (Davie Ridge, SW Indian Ocean). Terra Nova 30 (5), 380–388. https://doi.org/10.1111/ter.12353.

Darwin, C.R., 1842. The Structure and Distribution of Coral Reefs. Being the First Part of the Geology of the Voyage of the Beagle, under the Command of Capt. Fitzroy, R.N. During the Years 1832 to 1836. Smith Elder and Co., London.

Davis, J.K., Lawver, L.A., Norton, I.O., Gahagan, L.M., 2016. New Somali Basin magnetic anomalies and a plate model for the early Indian Ocean. Gondwana Res. 34, 16–28. https://doi.org/10.1016/j.gr.2016.02.010.

Debeuf, D., 2004. Etude de l'évolution volcano-structurale et magmatique de Mayotte (Archipel des Comores, Océan Indien): Approches structurale, pétrographique, géochimique et géochronologique. Unpublished Ph. D. thesis. Université de La Réunion, 243 pp.

Debeuf, D., 2011. Etude de l'évolution volcano-structurale et magmatique de Mayotte, Archipel des Comores, Océan Indien: approches structurale, pétrographique, géochimique et géochronologique. Volcanologie, 2009. Université de la Réunion, Français.

Denlinger, R.P., Morgan, J.K., 2014. Instability of Hawaiian volcanoes. In: Poland, M.P., Takahashi, T.J., Landowski, Claire M., M., C. (Eds.), Characteristics of Hawaiian Volcanoes Professional Paper 1801. U.S. Geological Survey, Reston, VA, USA, pp. 149–176.

Devey, C.W., Lackschewitz, K.S., Mertz, D.F., Bourdon, B., Cheminee, J.-L., Dubois, J., Guivel, C., Hekinian, R., Stoffers, P., 2003. Giving birth to hotspot volcanoes : distribution and composition of young seamounts from the seafloor near Tahiti and Pitcairn islands. Geology 31 (5), 395–398.

Deville, E., Marsset, T., Courgeon, S., Jatiault, R., Ponte, J.P., Thereau, E., Jouet, G., Jorry, S.J., Droz, L., 2018. Active fault system across the oceanic lithosphere of the Mozambique Channel: implications for the Nubia–Somalia southern plate boundary. Earth Planet. Sci. Lett. 502 https://doi.org/10.1016/j.epsl.2018.08.052.

Dieterich, J.H., 1988. Growth and persistence of Hawaiian volcanic rift zones. J. Geophys. Res. Solid Earth 93 (B5), 4258–4270.

Duffield, W.A., Bacon, C.R., Dalrympe, G.B., 1980. Late Cenozoic volcanism, geochronology, and structure of the Coso Range, Inyo County, California. J. Geophys. Res. 85, 2381–2404.

Dullo, W.C., Camoin, G.F., Blomeier, D., Colonna, M., Eisenhauer, A., Faure, G., Casanova, J., Thomassin, B.A., 1998. Morphology and sediments of the fore-slopes of Mayotte, Comoros Islands: direct observations from a submersible. In: Specialized Publication of the International Association of Sedimentologists, 25, pp. 219–236.

Emerick, C.M., 1985. Age Progressive Volcanism in the Comores Archipelago and Northern Madagascar. PhD thesis. Oregon State University, 195 pp.

Emerick, C.M., Duncan, R.A., 1982. Age progressive volcanism in the Comores Archipelago, Western Indian Ocean and implications for Somali Plate Tectonics. Earth Planet. Sci. Lett. 60 (3), 415–428.

Emmel, B., Kumar, R., Ueda, K., Jacobs, J., Daszinnies, M.C., Thomas, R.J., Matola, R., 2011. Thermochronological history of an orogen-passive margin system: an example from northern Mozambique. Tectonics 30, TC2002. https://doi.org/10.1029/2010TC002714.

Esson, J., Flower, M.F.J., Strong, D.F., Upton, B.G.J., Wadsworth, W.J., 1970. Geology of the Comores Archipelago, Western Indian Ocean. Geol. Mag. 107 (06), 549–557.

Famin, V., Michon, L., Bourhane, A., 2020. The Comoros archipelago: a right-lateral transform boundary between the Somalia and Lwandle plates. Tectonophysics. https://doi.org/10.1016/j.tecto.2020.228539.

Feuillet, N., Jorry, S.J., Crawford, W., Deplus, C., et al., 2019. Birth of a large volcano offshore Mayotte through lithosphere-scale rifting. In: AGU Fall Meeting, V52D-01, San Francisco.

Franke, D., Jokat, W., Ladage, S., Stollhofen, H., Klimke, J., Lutz, R., Mahanjane, E.S., Ehrhardt, A., Schreckenberger, B., 2015. The offshore east african rift system: structural framework at the toe of a Juvenile rift. Tectonics 34 (10). https://doi.org/10.1002/2015TC003922, 2015TC003922.

Gaffney, E.S., Damjanac, B., Valentine, G.A., 2007. Localization of volcanic activity: 2. Effects of preexisting structure. Earth Planet. Sci. Lett. 263, 323–338. https://doi.org/10.1016/j.epsl.2007.09.002.

Gee, M.J.R., Masson, D.G., Watts, A.B., Mitchell, N.C., 2001. Passage of debris flows and turbidity currents through a topographic constriction: seafloor erosion and deflection of pathways. Sedimentology 48, 1389–1409.

Geist, D.J., Fornari, D.J., Kurz, M.D., Harpp, K.S., Adam Soule, S., Perfit, M.R., Koleszar, A.M., 2006. Submarine Fernandina: Magmatism at the leading edge of the Galápagos hot spot. Geochem. Geophys. Geosyst. 7, Q12007 https://doi.org/10.1029/2006GC001290.

Geyer, A., Martí, J., 2010. The distribution of basaltic volcanism on tenerife, canary islands: implications on the origin and dynamics of the rift systems. Tectonophysics 483, 310–326. https://doi.org/10.1016/j.tecto.2009.11.002.

Guilcher, A., Berthois, L., Le Calvez, Y., Battistini, R., Crosnier, A., 1965. Les récifs coralliens et le lagon de l'île de Mayotte. In: Arch. Des Comores, Océan Indien. Mém. ORSTOM, n°11, 211 pp.

Hajash, A., Armstrong, R.L., 1972. Paleomagnetic and radiometric evidence for the age of the Comores islands, west central Indian Ocean. Earth Planet. Sci. Lett. 16 (2), 231–236. https://doi.org/10.1016/0012-821X(72)90195-1.

Hekinian, R., Cheminée, J.-L., Dubois, J., Stoffers, P., Scott, S., Guivel, C., Garbe-Schönberg, D., Devey, C., Bourdon, B., Lackschewitz, K., McMurtry, G., Le Drezen, E., 2003. The Pitcairn hotspot in the South Pacific: distribution and composition of submarine volcanic sequences. J. Volcanol. Geotherm. Res. 121, 219–245. https://doi.org/10.1016/S0377-0273(02)00427-4.

Holcomb, R.T., Searle, R.C., 1991. Large landslides from oceanic volcanoes. Mar. Geotechnol. 10 (1–2), 19–32. https://doi.org/10.1080/10641199109379880.

Huff, W.D., Owen, L.A., 2013. Volcanic landforms and hazards. In: Shroder, John F., Owen, L.A. (Eds.), Treatise on Geomorphology, Tectonic Geomorphology, 5. Academic Press, San Diego, pp. 148–192.

Hunt, J.E., Jarvis, I., 2017. Prodigious submarine landslides during the inception and early growth of volcanic islands. Nat. Commun. 8, 2061 (2017). https://doi.org/10.1038/s41467-017-02100-3.

Hunt, J.E., Talling, P.J., Clare, M.A., Jarvis, I., 2014. Long-term (17 Ma) turbidite record of the timing and frequency of large flank collapses of the Canary Islands. Geochem. Geophys. Geosyst. 15, 3322–3345.

Key, R.M., Smith, R.A., Smelror, M., Sæther, O.M., Thorsnes, T., Powell, J.H., Njange, F., Zandamela, E.B., 2008. Revised lithostratigraphy of the Mesozoic-Cenozoic succession of the onshore Rovuma Basin, northern coastal Mozambique. South Afr. J. Geol. 111, 89–108. https://doi.org/10.2113/gssajg.111.1.89.

Krastel, S., Schmincke, H.U., Jacobs, C.L., Rihm, R., Le Bas, T., Alibés, M., B., 2001a. Submarine landslides around the Canary Islands. J. Geophys. Res. 106 (B3), 3977–3997.

Krastel, S., Schmincke, H.U., Jacobs, C.L., 2001b. Formation of submarine canyons on the flanks of the Canary Islands. Geo-Mar. Lett. 20, 160–167. https://doi.org/10.1007/s003670000049.

Kusky, T.M., Toraman, E., Raharimahefa, T., Rasoazanamparany, C., 2010. Active tectonics of the Alaotra–Ankay Graben System, Madagascar: possible extension of Somalian–African diffusive plate boundary? Gondwana Res. 18, 274–294. https://doi.org/10.1016/j.gr.2010.02.003.

Lachassagne, P., Aunay, B., Frissant, N., Guilbert, M., Malard, A., 2014. High-resolution conceptual hydrogeological model of complex basaltic volcanic islands: a Mayotte, Comoros, case study. Terra Nova 26, 307–321. https://doi.org/10.1111/ter.12102.

Lacquement, F., Nehlig, P., Bernard, J., 2013. Carte géologique de Mayotte. BRGM. In: Report RP-61803-FR.

Le Friant, A., Lebas, E., Clément, V., Boudon, G., Deplus, C., de Voogd, B., Bachèlery, P., 2011. A new model for the evolution of La Réunion volcanic complex from complete marine geophysical surveys. Geophys. Res. Lett. 38, L09312 https://doi.org/10.1029/2011GL047489.

Lee, H.J., Syvitski, J.P.M., Parker, G., Orange, D., Locat, J., Hutton, E.W.H., Imran, J., 2002. Distinguishing sediment waves from slope failure deposits: field examples, including the "Humboldt Slide" and modeling results. Mar. Geol. 192, 79–104.

Lemoine, A., Briole, P., Bertil, D., Roullé, A., Foumelis, M., Thinon, I., Raucoules, D., de Michele, M., Valty, P., Hoste Colomer, R., 2020. The 2018–2019 seismo-volcanic crisis east of Mayotte, Comoros islands: seismicity and ground deformation markers of an exceptional submarine eruption. Geophys. J. Int. 223, 22–44.

Lénat, J.F., Bachèlery, P., Merle, O., 2012. Anatomy of Piton de la Fournaise Volcano (La Réunion, Indian Ocean). Bull. Volcanol. 74 (9), 1945–1961. https://doi.org/10.1007/s00445-012-0640-y.

Leroux, E., Counts, J., Jorry, S., Jouet, G., Révillon, S., BouDagher-Fadel, M.K., Courgeon, S., Berthod, C., Ruffet, G., Bachèlery, P., Grenard-Grand, E., 2020. Evolution of the Glorieuses seamount in the SW Indian ocean and surrounding deep Somali basin since the Cretaceous. Mar. Geol. 427 (2020), 106202. https://doi.org/10.1016/j.margeo.2020.106202.

MacDonald, G.A., 1972. Volcanoes. Prentice-Hall, Englewood Cliffs, NJ.

Macgregor, D., 2015. History of the development of the East African Rift System: a series of interpreted maps through time. J. Afr. Earth Sci. 101, 232–252.

Malod, J.A., Mougenot, D., Raillard, S., Maillard, A., 1991. New constraints on the kinematics of Madagascar - tectonic structures of the Davie ridge. Comp. Rendus Acad. Sci. Ser. II 312 (13), 1639–1646.

Masson, D.G., Watts, A.B., Gee, M.J.R., Urgeles, R., Mitchell, N.C., Le Bas, T.P., Canals, M., 2002. Slope failures on the flanks of the western Canary Islands. Earth-Sci. Rev. 57, 1–35.

Masson, D.G., Le Bas, T.P., Grevemeyer, I., Weinrebe, W., 2008. Flank collapse and large-scale landsliding in the Cape Verde Islands, off West Africa Masson. Geochem. Geophys. Geosyst. 9, Q07015 https://doi.org/10.1029/2008GC001983.

Mazuel, A., Sisavath, E., Babonneau, N., Jorry, S.J., Bachèlery, P., Delacourt, C., 2016. Turbidity current activity along the flanks of a volcanic edifice: the Mafate volcaniclastic complex, La Réunion Island, Indian Ocean. Sediment. Geol. 2016 (335), 34–50. Elsevier.

McGuire, W.J., 1996. Volcano instability: a review of contemporary themes. Geol. Soc. Lond., Spec. Publ. 110 (1), 1–23. https://doi.org/10.1144/GSL.SP.1996.110.01.01.

Medialdea, T., Somoza, L., Gonzalez, F.J., Vazquez, J.T., de Ignacio, C., Sumino, H., Sanchez-Guillamón, O., Orihashi, Y., Leon, R., Palomino, D., 2017. Evidence of a modern deep water magmatic hydrothermal system in the Canary Basin (eastern central Atlantic Ocean). Geochem. Geophys. Geosyst. 18, 3138–3164. https://doi.org/10.1002/2017GC006889.

Micallef, A., Mountjoy, J.J., 2011. A topographic signature of a hydrodynamic origin for submarine gullies. Geology 39, 115–118.

Michon, L., 2016. The volcanism of the Comoros Archipelago integrated at a regional scale. In: Active Volcanoes of the Southwest Indian Ocean, edited by Patrick Bachèlery, Jean-François Lénat, Andrea Di Muro, and Laurent Michon. Springer

Berlin Heidelberg, Berlin, Heidelberg, pp. 333–344. https://doi.org/10.1007/978-3-642-31395-0_21.
Mitchell, N.C., 2001. The transition from circular to stellate forms of submarine volcanoes. J. Geophys. Res. 106, 1987–2003.
Mitchell, N.C., 2003. Susceptibility of mid-ocean ridge volcanic islands and seamounts to large-scale landsliding. J. Geophys. Res. Solid Earth 108, 1–14.
Mitchell, N.C., Masson, D.G., Watts, A.B., Gee, M.J., Urgeles, R., 2002. The morphology of the submarine flanks of volcanic ocean islands: a comparative study of the Canary and Hawaiian hotspot islands. J. Volcanol. Geotherm. Res. 115, 83–107.
Mitchell, N.C., Strect, R., Oppenheimer, C., Kay, D., Beier, C., 2012. Cone morphology associated with shallow marine eruptions: east Pico Island. Azores. Bull. Volcanol. 74, 2289–2301.
Mitchell, N.C., Quartau, R., Madeira, J., 2013. Large-scale active slump of the southeastern flank of Pico Island, Azores: comment. Geology 41 (12), e301.
Montaggioni, L.F., Martin-Garin, B., 2020. Quaternary development history of coral reefs from West Indian islands: a review. Int. J. Earth Sci. 1–20.
Moore, J.G., 1964. Giant submarine landslides on the Hawaiian Ridge. In: Geological Survey Research: U.S. Geol. Survey Prof. Paper 501-D, pp. D95–D98.
Moore, J.G., Fiske, R.S., 1969. Volcanic substructure inferred from dredge samples and ocean-bottom photographs, Hawaii. Geol. Soc. Am. Bull. 80 (7), 1191–1202.
Moore, J.G., Clague, D.A., Holcomb, R.T., Lipman, P.W., Normark, W.R., Torresan, M.E., 1989. Prodigious submarine landslides on the Hawaiian ridge. J. Geophys. Res. 94, 17465–17484.
Moore, J.G., Normark, W.R., Holcomb, R.T., 1994. Giant Hawaiian landslides. Annu. Rev. Earth Planet. Sci. 22 (1994), 119–144.
Morgan, W.J., 1972. Deep mantle convection: plumes and plate motions. Am. Ass. Petrol. Geol. Bull. 56, 203–213.
Morgan, J.K., Moore, G.F., Clague, D.A., 2003. Slope failure and volcanic spreading along the submarine south flank of Kilauea volcano, Hawaii. J. Geophys. Res. 108 (B9), 2415. https://doi.org/10.1029/2003JB002411.
Mougenot, D., Recq, M., Virlogeux, P., Lepvrier, C., 1986. Seaward extension of the East-African Rift. Nature 321 (6070), 599–603. https://doi.org/10.1038/321599a0.
Mpanda, S., 1997. Geological Development of the East African Coastal Basin of Tanzania.
Mueller, C.O., Jokat, W., 2019. The initial Gondwana break-up; a synthesis based on new potential field data of the Africa-Antarctica corridor. Tectonophysics 750, 301–328.
Muffler, L.J.P., Clynne, M.A., Calvert, A.T., Champion, D.E., 2011. Diverse, discrete, mantle-derived batches of basalt erupted along a short normal fault zone : the poison Lake chain, southernmost Cascades. Geol. Soc. Am. Bull. 123 (11−12), 2177–2200. https://doi.org/10.1130/b30370.1.
Mulder, T., 2011. (4.2.3) Depositional bedforms: sediment waves. In: Deep-Sea Sediments, Developments in Sedimentology, 63. https://doi.org/10.1016/B978-0-444-53000-4.00010-X. Pages 715-764, Edited by Heiko HüNeke, Thierry Mulder.
Nehlig, P., Lacquement, F., Bernard, J., Caroff, M., Deparis, J., Jaouen, T., Pelleter, A., Perrin, J., Prognon, C., Vittecoq, B., 2013. Notice de la carte géologique de Mayotte BRGM/RP-61803-FR, 143pp, 45 fig., 1 ann.
Németh, K., Kereszturi, G., 2015. Monogenetic volcanism: personal views and discussion. Int. J. Earth Sci. 104, 2131–2146.
Neves, M.C., Miranda, J.M., Luis, J.F., 2013. The role of lithospheric processes on the development of linear volcanic ridges in the Azores. Tectonophysics 608, 376–388.
Nougier, J., Cantagrel, J.M., Karche, J.P., 1986. The Comores Archipelago in the Western Indian Ocean: volcanology, geochronology and geodynamic setting. J. Afr. Earth Sci. 5 (2), 135–144. https://doi.org/10.1016/0899-5362(86)90003-5.
O'Connor, J.M., Jokat, W., Regelous, M., et al., 2019. Superplume mantle tracked isotopically the length of Africa from the Indian Ocean to the Red Sea. Nat. Commun. 10, 5493. https://doi.org/10.1038/s41467-019-13181-7.
Oehler, J.F., Lénat, J.F., Labazuy, P., 2008. Growth and collapse of the Reunion Island volcanoes. Bull. Volcanol. 70 (2008), 717–742. https://doi.org/10.1007/s00445-007-0163-0.
Paquet, F., Jorry, S., Deplus, C., Le Friant, A., Julien, B., Bremell-Fleury, S., Feuillet, N., Gaillot, A., Guérin, C., Thinon, I., 2019. The Mayotte Seismo-volcanic crisis: characterizing a reactivated volcanic ridge from the upper slope to the abyssal plain using multibeam bathymetry and backscatter data. In: Proceedings of the AGU Fall Meeting 2019. AGU.
Pelleter, A.A., Caroff, M., Cordier, C., Bachèlery, P., Nehlig, P., Debeuf, D., Arnaud, N., 2014. Melilite-bearing lavas in Mayotte (France): an insight into the mantle source below the Comores. Lithos (208–209), 281–297. https://doi.org/10.1016/j.lithos.2014.09.012.
Postma, G., Cartigny, M., 2014. Supercritical and subcritical turbidity currents and their deposits- a synthesis. Geology 42, 987–990.
Puga-Bernabéu, A., Webster, J.M., Braga, J.C., Clague, D.A., Dutton, A., Eggins, S., Fallon, S., Jacobsen, G., Paduan, J.B., Potts, D.C., 2016. Morphology and evolution of drowned carbonate terraces during the last two interglacial cycles, off Hilo, NE Hawaii. Mar. Geol. 371, 57–81. https://doi.org/10.1016/j.margeo.2015.10.016.
Quartau, R., Trenhaile, A.S., Mitchell, N.C., Tempera, F., 2010. Development of volcanic insular shelves: insights from observations and modelling of Faial Island in the Azores Archipelago. Mar. Geol. 275, 66–83.
Quartau, R., Hipólito, A., Romagnoli, C., Casalbore, D., Madeira, J., Tempera, F., Chiocci, F.L., 2014. The morphology of insular shelves as a key for understanding the geological evolution of volcanic islands: insights from Terceira Island (Azores). Geochemistry, Geophysics, Geosystems 15 (5), 1801–1826.
Raillard, S., 1990. Les marges de l'Afrique de l'est et les zones de fracture associées. In: Chaine Davie et Ride du Mozambique. Campagne MD-60/MACAMO-1I. Thèse d'Université Univ. P. et M. Curie, Paris, 272 pp.
Ramalho, R.S., Quartau, R., Trenhaile, A.S., Mitchell, N.C., Woodroffe, C.D., Ávila, S.P., 2013. Coastal evolution on volcanic oceanic islands: a complex interplay between volcanism, erosion, sedimentation, sea-level change and biogenic production. Earth-Sci. Rev. 127 (2013), 140–170. https://doi.org/10.1016/j.earscirev.2013.10.007.
Ricchi, A., Quartau, R., Ramalho, R.S., Romagnoli, C., Casalbore, D., Ventura da Cruz, J., Fradique, C., Vinhas, A., 2018. Marine terrace development on reefless volcanic islands: New insights from high-resolution marine geophysical data offshore Santa Maria Island (Azores Archipelago). Mar. Geol. 406, 42–56. https://doi.org/10.1016/j.margeo.2018.09.002.
Ricchi, A., Quartau, R., Ramalho, R.S., Romagnoli, C., Casalbore, D., Zhao, Z., 2020. Imprints of volcanic, erosional, depositional, tectonic and mass-wasting processes in the morphology of Santa Maria insular shelf (Azores). Mar. Geol. 424 (June 2020) https://doi.org/10.1016/j.margeo.2020.106163.
Rindraharisaona, E.J., Guidarelli, M., Aoudia, A., Rambolamanana, G., 2013. Earth structure and instrumental of Madagascar: implications on the seismotectonics. Tectonophysics 594, 165–181. https://doi.org/10.1016/j.tecto. 2013.03.033.
Romagnoli, C., Casalbore, D., Chiocci, F.L., Bosman, A., 2009. Off-shore evidence of large-scale lateral collapses on the eastern flank of Stromboli, Italy, due to structurally-controlled, bilateral flank instability. Mar. Geol. 262, 1–13. https://doi.org/10.1016/j.margeo.2009.02.004.
Romagnoli, C., Casalbore, D., Bosman, A., Braga, R., Chiocci, F.L., 2013. Submarine structure of Vulcano volcano (Aeolian Islands) revealed by high-resolution bathymetry and seismo-acoustic data. Mar. Geol. 338, 30–45.
Romagnoli, C., Casalbore, D., Ricchi, A., Lucchi, F., Quartau, R., Bosman, A., Chiocci, F. L., 2018. Morpho-bathymetric and seismo-stratigraphic analysis of the insular shelf of Salina (Aeolian archipelago) to unveil its Late-Quaternary geological evolution. Marine Geology 395, 133–151.
Romagnoli, C., Belvisi, V., Innangi, S., Di Martino, G., Tonielli, R., 2020. New insights on the evolution of the Linosa volcano (Sicily Channel) from the study of its submarine portions. Mar. Geol. 419 (2020), 1–12.
Romero Ruiz, C., García-Cacho, L., Araña, V., Yanes Luque, A., Felpeto, A., 2000. Submarine volcanism surrounding Tenerife, Canary Islands: implications for tectonic controls, and oceanic shield forming processes. J. Volcanol. Geotherm. Res. 103, 105–119.
Rubin, K.H., Soule, S.A., Chadwick Jr., W.W., Fornari, D.J., Clague, D.A., Embley, R.W., Baker, E.T., Perfit, M.R., Caress, D.W., Dziak, R.P., 2012. Volcanic eruptions in the deep sea. Oceanography 25 (1), 142–157. https://doi.org/10.5670/oceanog.2012.12.
Saint-Ange, F., Bachèlery, P., Babonneau, N., Michon, L., Jorry, S.J., 2013. Volcaniclastic sedimentation on the submarine slopes of a basaltic hotspot volcano: Piton de la Fournaise volcano (La Réunion Island, Indian Ocean). Mar. Geol. 337, 35–52. https://doi.org/10.1016/j.margeo.2013.01.004.
Sanchez-Guillamón, O., Vázquez, J.T., Palomino, D., Medialdea, T., Fernández-Salas, L. M., León, R., Somoza, L., 2018. Morphology and shallow structure of seafloor mounds in the Canary Basin (Eastern Central Atlantic Ocean). Geomorphology 313 (2018), 27–47.
Schlager, W., Camber, O., 1986. Submarine slope angles, drowning unconformities, and self-erosion of limestone escarpments. Geology 14, 762–765.
Segoufin, J., Patriat, P., 1980. Existences d'anomalies mésozoïques dans le bassin de Somalie: implications pour les relations Afrique-Antarctique-Madagascar. C.R. Acad. Sci. 291 (1980), 85–88.
Sisavath, E., Babonneau, N., Saint-Ange, F., Bachèlery, P., Jorry, S.J., Deplus, C., de Voogd, B., Savoye, B., 2011. Morphology and sedimentary architecture of a modern volcaniclastic turbidite system: the Cilaos fan, offshore La Réunion Island. Mar. Geol. 288 (2011), 1–17. https://doi.org/10.1016/j.margeo.2011.06.011. Ticket 1-4.
Smith, I.E.M., Németh, K., 2017. Source to Surface Model of Monogenetic Volcanism: A Critical Review, 446. Geological Society, London, Special Publications, pp. 1–28, 31 March 2017. https://doi.org/10.1144/SP446.14.
Späth, A., LeRoex, A.P., Duncan, R.A., 1996. The Geochemistry of Lavas from the Comores Archipelago, Western Indian Ocean: Petrogenesis and Mantle Source Region Characteristics. J. Petrol. 37 (4), 961–991. https://doi.org/10.1093/petrology/37.4.961.
Spiess, F.N., Luyendyk, B.P., Larson, R.L., Normark, W.R., Mudie, J.D., 1969. Detailed geophysical studies on the northern Hawaiian Arch using a deeply towed instrument package. Mar. Geol. 7 (6), 501–527.
Stamps, D.S., Saria, E., Kreemer, C., 2018. A geodetic strain rate model for the east African rift system. Sci. Rep. 8, 732. https://doi.org/10.1038/s41598-017-19097-w.
Staudigel, H., Koppers, A.A.P., 2015. Seamounts and island building. In: Sigurdsson, H., Houghton, B., McNutt, S., Rymer, H., Stix, J. (Eds.), The Encyclopedia of Volcanoes, 2nd edition. Academic Press, pp. 405–422.
Stretch, R.C., Mitchell, N., Portaro, R.A., 2006. A morphometric analysis of the submarine volcanic ridge south-east of Pico Island, Azores. J. Volcanol. Geotherm. Res. 156 (1), 35–54. https://doi.org/10.1016/j.jvolgeores.2006.03.009.
Thompson, J.O., Moulin, M., Aslanian, D., de Clarens, P., Guillocheau, F., 2019. New starting point for the Indian Ocean: second phase of breakup for Gondwana. Earth Sci. Rev. 1991, 26–56. https://doi.org/10.1016/j.earscirev.2019.01.018.
Tilling, R.I., Dvorak, J.J., 1993. Anatomy of a basaltic volcano. Nature 363 (6425), 125–133.
Upton, B.G.J., 1982. Oceanic Islands. In: Nairn, P., Stehli, F. (Eds.), Ocean Basins and their Margins, Indian Ocean, 6(13). Plenum Press, New York, pp. 585–648.
Valentine, G.A., Krogh, K.E.C., 2006. Emplacement of shallow dikes and sills beneath a small basaltic volcanic center—the role of pre-existing structure (Paiute Ridge, southern Nevada, USA). Earth Planet. Sci. Lett. 246, 217–230. https://doi.org/10.1016/j.epsl.2006.04.031.
Vittecoq, B., Deparis, J., Violette, S., Jaouën, T., Lacquement, F., 2014. Influence of successive phases of volcanic construction and erosion on Mayotte Island's hydrogeological functioning as determined from a helicopter-borne resistivity survey correlated with borehole geological and permeability data. J. Hydrol. 509, 519–538.

Wanless, V.D., Garcia, M.O., Trusdell, F.A., Rhodes, J.M., Norman, M.D., Weis, D., 2006. Submarine radial vents on Mauna Loa Volcano Hawai'i. Geochem. Geophys. Geosyst. 7 (5), 1–28. https://doi.org/10.1029/2005GC001086.

Weiß, B.J., Huebscher, C., Ludmann, T., 2015. The Tectonic Evolution of the South-Eastern Terceira Rift / São Miguel Region (Azores). Tectonophysics 654. https://doi.org/10.1016/j.tecto.2015.04.018.

Wynn, R.B., Piper, D.J.W., Gee, M.J.R., 2002. Generation and migration of coarse-grained sediment waves in turbidity current channels and channel–lobe transition zones. Mar. Geol. 192, 59–78.

Zinke, J., Reijmer, J.J.G., Dullo, W.-Ch., Thomassin, B.A., 2003a. Systems tracts sedimentology in the lagoon of Mayotte associated with the Holocene transgression. Sediment. Geol. 160, 57–79.

Zinke, J., Reijmer, J.J.G., Thomassin, B.A., Dullo, W.-Chr., Grootes, P.M., Erlenkeuser, H., 2003b. Postglacial flooding history of Mayotte Lagoon (Comoro Archipelago, Southwest Indian Ocean). Mar. Geol. 194 (3–4), 181–196. https://doi.org/10.1016/S0025-3227(02)00705-3.

Zinke, J., Reijmer, J.J.G., Taviani, M., Dullo, W.-Chr., Thomassin, B.A., 2005. Facies and faunal assemblage changes in response to the Holocene transgression in the Holocene transgression in the Lagoon of Mayotte (Comoro Archipelago, SW Indian Ocean). Facies 50, 391–408. https://doi.org/10.1007/s10347-004-0040-7.